NATIONAL ADVISORY COMMITTEE FOR AERONAUTICS

NACA-TR-633

REPORT No. 633

PRESSURE DISTRIBUTION OVER AN N. A. C. A. 23012 AIRFOIL WITH A SLOTTED AND A PLAIN FLAP

By CARL J. WENZINGER and JAMES B. DELANO

1938

AERONAUTIC SYMBOLS

1. FUNDAMENTAL AND DERIVED UNITS

	Symbol	Metric		English	
		Unit	Abbreviation	Unit	Abbreviation
Length	l	meter	m	foot (or mile)	ft. (or mi.)
Time	t	second	s	second (or hour)	sec. (or hr.)
Force	F	weight of 1 kilogram	kg	weight of 1 pound	lb.
Power	P	horsepower (metric)		horsepower	hp.
Speed	V	{kilometers per hour	k.p.h.	miles per hour	m.p.h.
		{meters per second	m.p.s.	feet per second	f.p.s.

2. GENERAL SYMBOLS

W, Weight $=mg$

g, Standard acceleration of gravity $=9.80665$ m/s^2 or 32.1740 ft./sec.^{2}

m, Mass $=\frac{W}{g}$

I, Moment of inertia $=mk^2$. (Indicate axis of radius of gyration k by proper subscript.)

μ, Coefficient of viscosity

ν, Kinematic viscosity

ρ, Density (mass per unit volume)

Standard density of dry air, 0.12497 kg-m^{-4}-s^2 at 15° C. and 760 mm; or 0.002378 lb.-ft.$^{-4}$ sec.^{2}

Specific weight of "standard" air, 1.2255 kg/m^3 or 0.07651 lb./cu. ft.

3. AERODYNAMIC SYMBOLS

S, Area

S_w, Area of wing

G, Gap

b, Span

c, Chord

$\frac{b^2}{S}$, Aspect ratio

V, True air speed

q, Dynamic pressure $=\frac{1}{2}\rho V^2$

L, Lift, absolute coefficient $C_L=\frac{L}{qS}$

D, Drag, absolute coefficient $C_D=\frac{D}{qS}$

D_0, Profile drag, absolute coefficient $C_{D_0}=\frac{D_0}{qS}$

D_i, Induced drag, absolute coefficient $C_{D_i}=\frac{D_i}{qS}$

D_p, Parasite drag, absolute coefficient $C_{D_p}=\frac{D_p}{qS}$

C, Cross-wind force, absolute coefficient $C_C=\frac{C}{qS}$

R, Resultant force

i_w, Angle of setting of wings (relative to thrust line)

i_t, Angle of stabilizer setting (relative to thrust line)

Q, Resultant moment

Ω, Resultant angular velocity

$\rho\frac{Vl}{\mu}$, Reynolds Number, where l is a linear dimension (e.g., for a model airfoil 3 in. chord, 100 m.p.h. normal pressure at 15° C., the corresponding number is 234,000; or for a model of 10 cm chord, 40 m.p.s., the corresponding number is 274,000)

C_p, Center-of-pressure coefficient (ratio of distance of c.p. from leading edge to chord length)

α, Angle of attack

ϵ, Angle of downwash

α_0, Angle of attack, infinite aspect ratio

α_i, Angle of attack, induced

α_a, Angle of attack, absolute (measured from zero-lift position)

γ, Flight-path angle

REPORT No. 633

PRESSURE DISTRIBUTION OVER AN N. A. C. A. 23012 AIRFOIL WITH A SLOTTED AND A PLAIN FLAP

By CARL J. WENZINGER and JAMES B. DELANO

Langley Memorial Aeronautical Laboratory

74939—38——1

NATIONAL ADVISORY COMMITTEE FOR AERONAUTICS

HEADQUARTERS, NAVY BUILDING, WASHINGTON, D. C.

LABORATORIES, LANGLEY FIELD, VA.

Created by act of Congress approved March 3, 1915, for the supervision and direction of the scientific study of the problems of flight (U. S. Code, Title 50, Sec. 151). Its membership was increased to 15 by act approved March 2, 1929. The members are appointed by the President, and serve as such without compensation.

TECHNICAL COMMITTEES

AERODYNAMICS
POWER PLANTS FOR AIRCRAFT
AIRCRAFT MATERIALS
AIRCRAFT STRUCTURES
AIRCRAFT ACCIDENTS
INVENTIONS AND DESIGNS

Coordination of Research Needs of Military and Civil Aviation

Preparation of Research Programs

Allocation of Problems

Prevention of Duplication

Consideration of Inventions

LANGLEY MEMORIAL AERONAUTICAL LABORATORY

LANGLEY FIELD, VA.

Unified conduct, for all agencies, of scientific research on the fundamental problems of flight.

OFFICE OF AERONAUTICAL INTELLIGENCE

WASHINGTON, D. C.

Collection, classification, compilation, and dissemination of scientific and technical information on aeronautics.

REPORT No. 633

PRESSURE DISTRIBUTION OVER AN N. A. C. A. 23012 AIRFOIL WITH A SLOTTED AND A PLAIN FLAP

By Carl J. Wenzinger and James B. Delano

SUMMARY

Pressure-distribution tests of an N. A. C. A. 23012 airfoil equipped with a slotted flap and with a plain flap were made in the 7- by 10-foot wind tunnel. A test installation was used in which the 7-foot-span airfoil was mounted vertically between the upper and lower sides of the closed test section so that two-dimensional flow was approximated. The pressures were measured on the upper and lower surfaces at one chord section both on the main airfoil and on the flaps for several different flap deflections and at several angles of attack.

The data are presented in the form of pressure-distribution diagrams and as graphs of calculated section coefficients for the airfoil-and-flap combinations and also for the flaps alone. The results are useful for application to rib and flap structural design; in addition, the plain-flap data furnish considerable information applicable to the structural design of plain ailerons.

INTRODUCTION

Up to the present time, many high-lift devices have been developed and investigated, but each appears to have some disadvantages. One of the most promising high-lift devices thus far developed is the combination of a slotted flap with a main airfoil. Investigations of this arrangement (reference 1) have shown that it is capable of developing high lifts and that it gives lower drags at these high lifts than do external-airfoil, plain, or split flaps.

The force tests of reference 1, in which several combinations of an N. A. C. A. 23012 airfoil with flaps of different sections and with slots of several different shapes were investigated, indicated that the best arrangement thus far obtained is a combination of an airfoil and a slotted flap, the flap having an airfoil shape and the slot an easy entrance; this combination is designated flap 2-h in reference 1. A survey of flap location with respect to the main airfoil was made to obtain the best aerodynamic characteristics. It was also found that some particular flap path would give optimum aerodynamic characteristics; the flap path developed is reported in reference 1.

Very few data are available for application to the structural design of slotted flaps. Some recent data (references 2 and 3) are available but, as the reported tests were not very comprehensive, the present investigation was undertaken to supply information applicable to the structural design of slotted flaps. Similar data are already available for the design of split, external-airfoil, and Fowler flaps (references 4, 5, and 6).

Pressure-distribution tests were made in the 7- by 10-foot wind tunnel of an N. A. C. A. 23012 airfoil in combination with a slotted flap. The optimum flap path previously developed for this flap (reference 1) was used in these tests. Pressure-distribution tests were also made over the same airfoil in combination with a plain flap for purposes of comparison and also to obtain additional information for the detailed structural design of both flaps and ailerons.

APPARATUS AND TESTS

MODELS

The models used in the present tests are the ones previously used in the force tests reported in reference 1. The main airfoil, made of laminated pine to the N. A. C. A. 23012 profile, has a uniform chord of 3 feet and a span of 7 feet. A removable full-span trailing-edge section permits the testing of different full-span flaps in combination with the same main airfoil. Both a slotted flap and a plain flap made of laminated pine were tested; each was supported on the main airfoil by three metal fittings, one located at mid-span and one inboard of each flap tip.

The slotted flap tested (fig. 1) is the one previously developed by the N. A. C. A. and designated 2–h in reference 1; it has a chord of 9.238 inches (25.66 percent of the over-all airfoil chord). A full-span fixed lip made of strip brass is located on the upper surface of the main airfoil over the flap-slot exit to seal the slot when the flap is neutral and to direct the passage of air downward over the flap when the flap is deflected. The path of the nose point of the flap chosen (fig. 1) is the optimum one reported in the tests described in reference 1. The nose point of the flap is defined as the point of tangency of a line drawn normal to the airfoil chord and tangent to the leading-edge arc of the flap when neutral. The flap is arranged for locking at downward flap deflections between 0° and 60° in increments of 10°.

The plain flap (fig. 1) has a chord of 7.20 inches (20.0 percent of the over-all airfoil chord). The flap gap was sealed for all flap deflections by interchangeable full-span brass lips on the upper and lower surfaces of the airfoil to prevent a flow of air through the gap. The flap is arranged for locking at flap deflections between 45° up and 75° down in increments of 15°.

A single row of pressure orifices was built into the upper and lower surfaces of both the main airfoil and the flaps at a chord section 21 inches from one end of the models (fig. 2). The orifices were located on the models as listed in table I, the tubes from the orifices being brought through the models and out at one end. The pressures were photographically recorded by a multiple-tube liquid manometer.

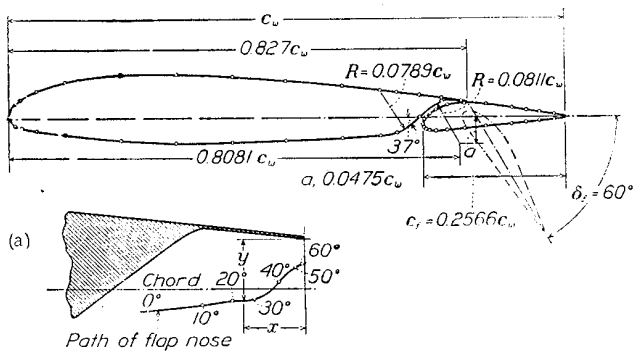

(a) N. A. C. A. 23012 airfoil with a $0.2566c_w$ slotted flap.

δ_f (deg.)	Path of flap nose for various flap deflections. Distances measured from lower edge of lip in percent airfoil chord c_w	
	x	y
0	8.36	3.91
10	5.41	3.63
20	3.83	3.45
30	2.63	3.37
40	1.35	2.43
50	.50	1.63
60	.12	1.48

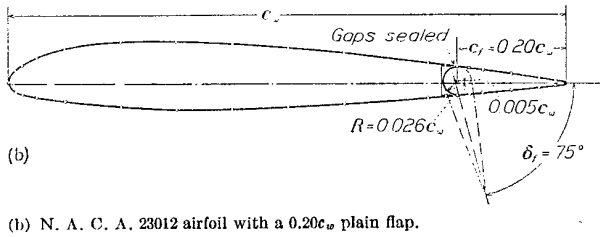

(b) N. A. C. A. 23012 airfoil with a $0.20c_w$ plain flap.

FIGURE 1.—Cross sections of model showing airfoil-flap combinations used in pressure-distribution tests.

TEST INSTALLATION

The model was mounted in the N. A. C. A. 7- by 10-foot closed-jet wind tunnel (references 1 and 7) as indicated in figure 2. The main airfoil was rigidly attached to the balance frame by torque tubes, which extended through the upper and lower sides of the tunnel. The angle of attack of the model was set from outside the tunnel by rotating the torque tubes with a calibrated electric drive. Approximately two-dimensional flow is obtained with this type of installation, and the section characteristics of the model under test may be determined.

TESTS

All the tests were made at a dynamic pressure of 16.37 pounds per square foot, corresponding to an air

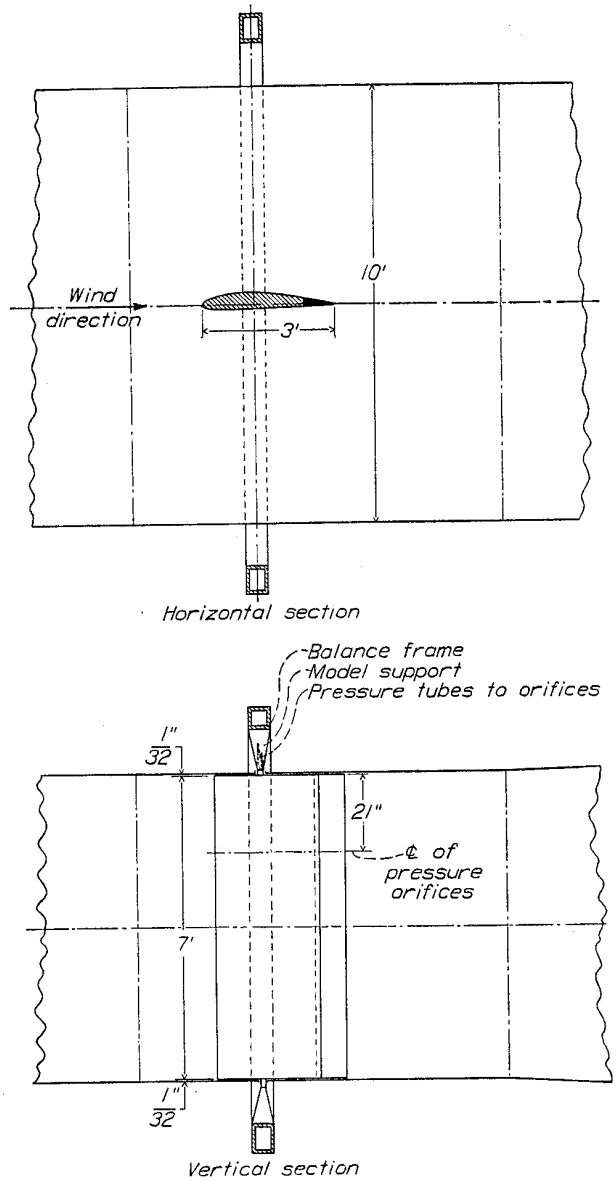

FIGURE 2.—Model installation for two-dimensional flow tests in the 7- by 10-foot wind tunnel.

speed of about 80 miles per hour at standard sea-level conditions. The average test Reynolds Number, based on the plain airfoil chord, was 2,190,000. This test Reynolds Number, when converted to an effective Reynolds Number (reference 8) that takes account of the turbulence in the air stream, is 3,500,000. (Effective Reynolds Number=average test Reynolds Number×turbulence factor; turbulence factor for the tunnel is 1.6.)

The model was tested with the slotted flap set at angles of 0°, 10°, 20°, 30°, 40°, 50°, and 60° down; and with the plain flap set at angles of 45°, 30°, and 15° up, 0°, and 15°, 30°, 45°, 60°, and 75° down. The angles of attack ranged from −14° to 20°, and the lift coefficients included those from approximately maximum negative to maximum positive. With the model at a given angle of attack and with a given flap setting, tunnel conditions were allowed to become steady before a record of the pressures at the orifices was taken.

PRESENTATION OF DATA

PRESSURE DIAGRAMS

All diagrams of pressures over the upper and lower surfaces of the airfoil-flap combinations are given as ratios of the orifice pressure p to the dynamic pressure q of the free air stream for the flap deflections and for the angles of attack investigated. Pressure diagrams for the airfoil with the slotted flap are shown in figures 3 to 15 and, for the airfoil with the plain flap, in figures 16 to 24. The effect of the flaps on the pressure distribution over the main airfoil is shown by a comparison of the pressures over the plain airfoil with the pressures over both the slotted-flap and the plain-flap combinations at the same total normal-force coefficient and also at the same angle of attack (figs. 25 and 26). In figures 3 to 9 and 16 to 26, the pressures over the main airfoil are plotted normal to the airfoil chord and the pressures over the flaps are plotted normal to a reference line which is parallel to the main airfoil chord when the flap is neutral but which deflects with the flap.

Figures 10 to 15 are included to show the pressures parallel to the chord of the slotted flap. These pressures are also given as ratios of orifice pressure to the dynamic pressure of the air stream; however, the pressure values are plotted parallel to, instead of normal to, the flap reference line and are measured from the maximum ordinates of the flap instead of from its reference line.

COEFFICIENTS

The pressure diagrams were mechanically integrated to obtain data from which section coefficients were computed. Where the term "flap alone" is used, reference is made to the characteristics of the flap in the presence of the main airfoil. The section coefficients are defined as follows:

$c_{n_w}=\frac{n_w}{qc_w}$, normal-force coefficient of main airfoil with flap.

$c_{n_f}=\frac{n_f}{qc_f}$, normal-force coefficient of flap alone.

$c_{m_w}=\frac{m_w}{qc_w^2}$, pitching-moment coefficient of main airfoil with flap about quarter-chord point of airfoil.

$c_{m_f}=\frac{m_f}{qc_f^2}$, pitching-moment coefficient of slotted flap alone about quarter-chord point of flap.

$c_{h_f}=\frac{h_f}{qc_f^2}$, hinge-moment coefficient of plain flap about flap hinge axis.

$c_{c_f}=\frac{x_f}{qc_f}$, chord-force coefficient of slotted flap alone.

$(c.\ p.)_w=\left(0.25-\frac{c_{m_w}}{c_{n_w}}\right)\times 100$, center-of-pressure location of main airfoil with flap in percent airfoil chord from leading edge.

$(c.\ p.)_f=\left(0.25-\frac{c_{m_f}}{c_{n_f}}\right)\times 100$, center-of-pressure location of flap alone in percent flap chord from leading edge of flap.

where the forces and moments per unit span are:

n_w, normal force on main airfoil with flap (this force is normal to chord of main airfoil and is equal to $n_m+n_f\cos\delta_f$, neglecting the normal component of the flap chord force).

n_m, normal force on main portion of the airfoil without flap (this force is normal to chord of main airfoil and is equal to $n_w-n_f\cos\delta_f$).

n_f, normal force on flap alone normal to chord of flap.

m_w, pitching moment of main airfoil with flap about quarter-chord point of airfoil.

m_f, pitching moment of slotted flap about quarter-chord point of flap.

h_f, hinge moment of plain flap.

x_f, chord force on slotted flap alone.

and

q, dynamic pressure of free air stream.

c_w, chord of main airfoil.

c_f, chord of flap.

The coefficients for the combination were derived from the normal forces alone, the chord forces of the flaps being neglected. In the case of the slotted flap, however, neglecting the flap chord-force component in the computation of the total normal-force coefficient of the combination reduces these coefficients by a maximum of about 0.08.

Because the model completely spanned the jet, the integrated results, which are given in coefficient form in figures 27 to 42, may be taken to be section characteristics. The normal-force coefficients of the airfoil-flap combinations include an experimentally determined correction for tunnel-wall effects, which was made as in reference 1.

PRECISION

No air-flow alinement tests were made in the wind tunnel with the test arrangement used in this investigation, so the absolute angle of attack may be slightly in error; the relative angles are correct to within ±0.1°. The flaps were set to specified angles to within ±0.1°. The orifice pressures, based on check tests in which both the angle of attack and the flap setting were independently changed, show that they agreed to within ±2 percent, with the exception of upper-surface

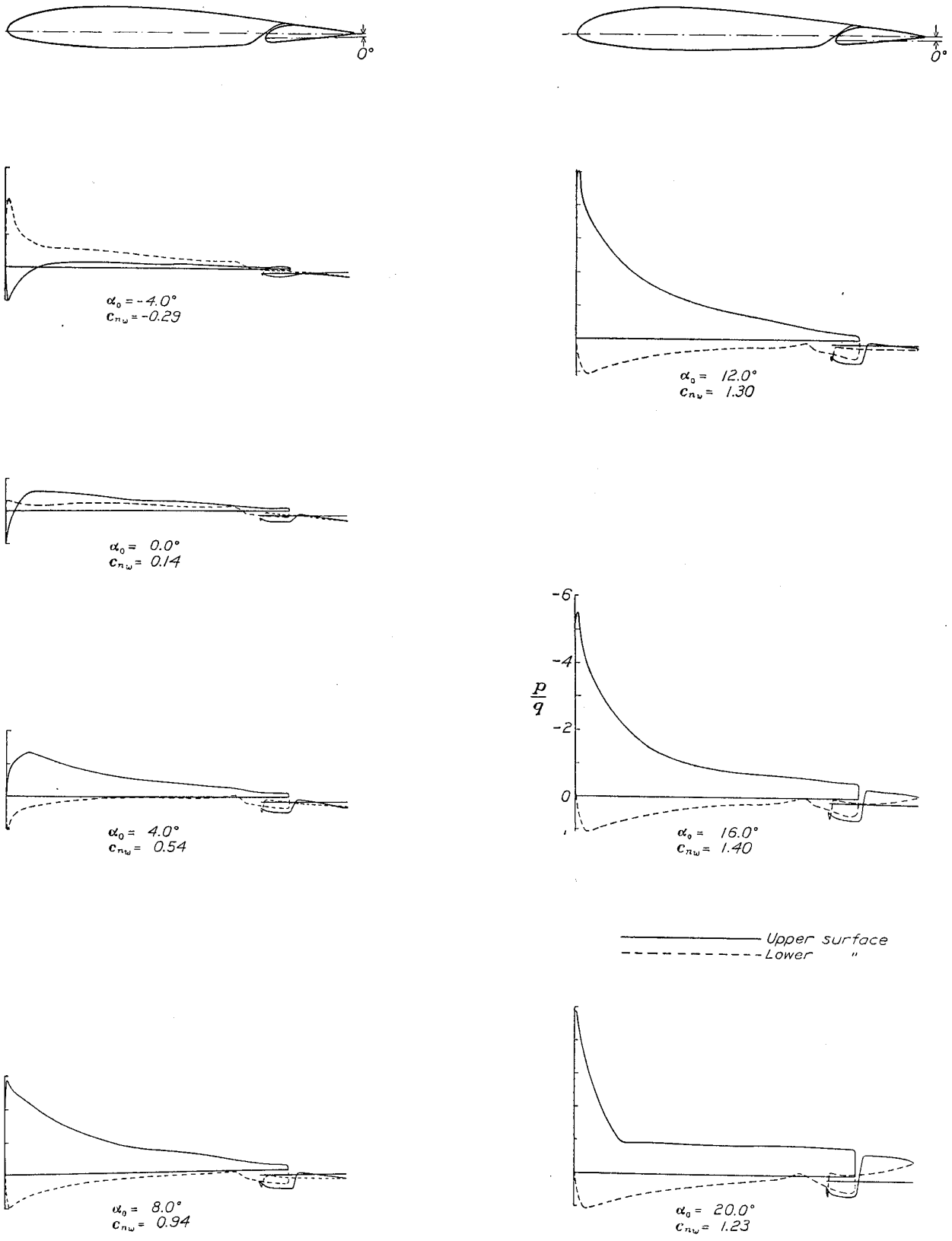

FIGURE 3.—Pressure distribution on the N. A. C. A. 23012 airfoil with a $0.2566c_w$ slotted flap, at various angles of attack. Flap set at 0°.

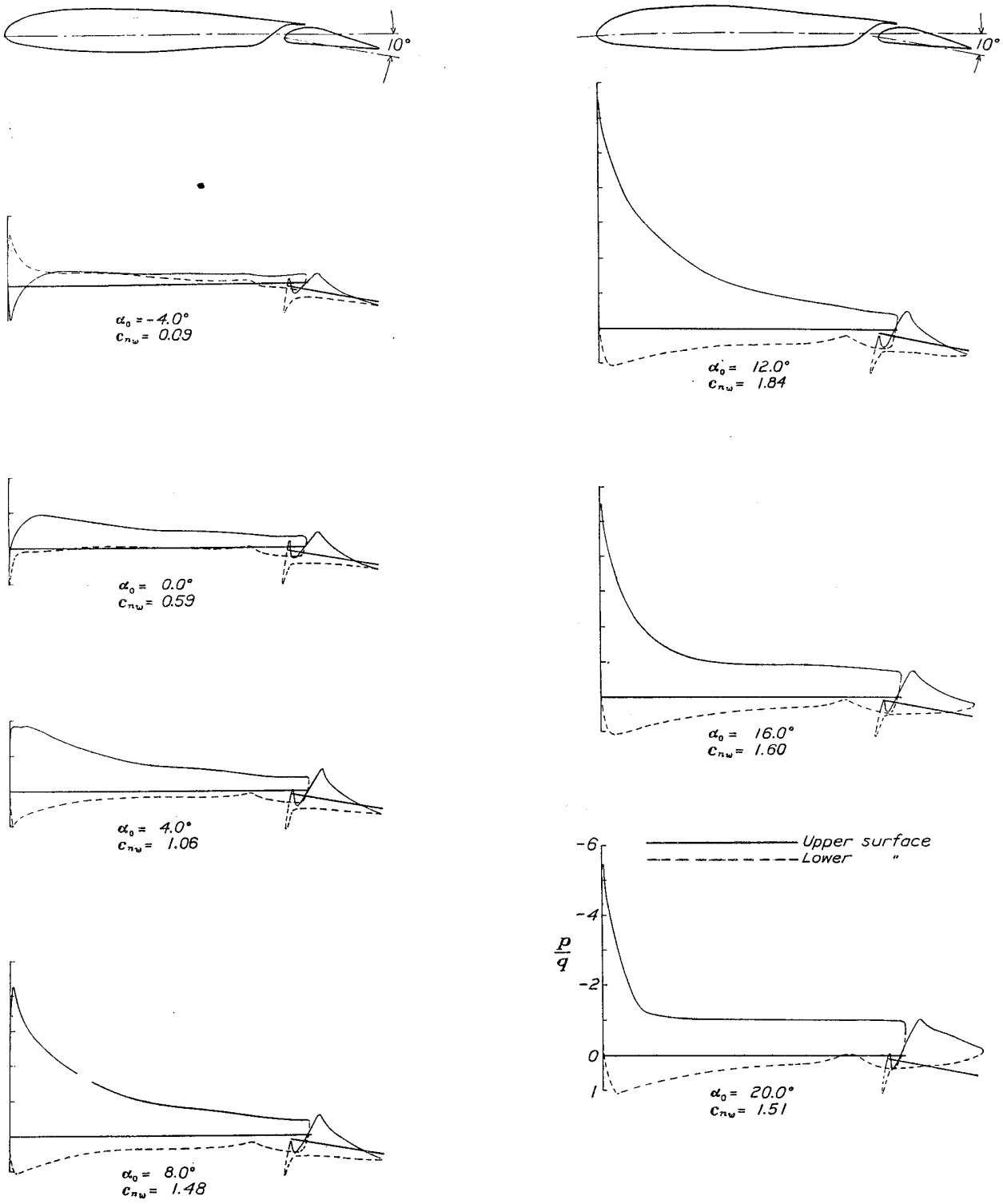

FIGURE 4.—Pressure distribution on the N. A. C. A. 23012 airfoil with a $0.2566c_w$ slotted flap, at various angles of attack. Flap set at 10°.

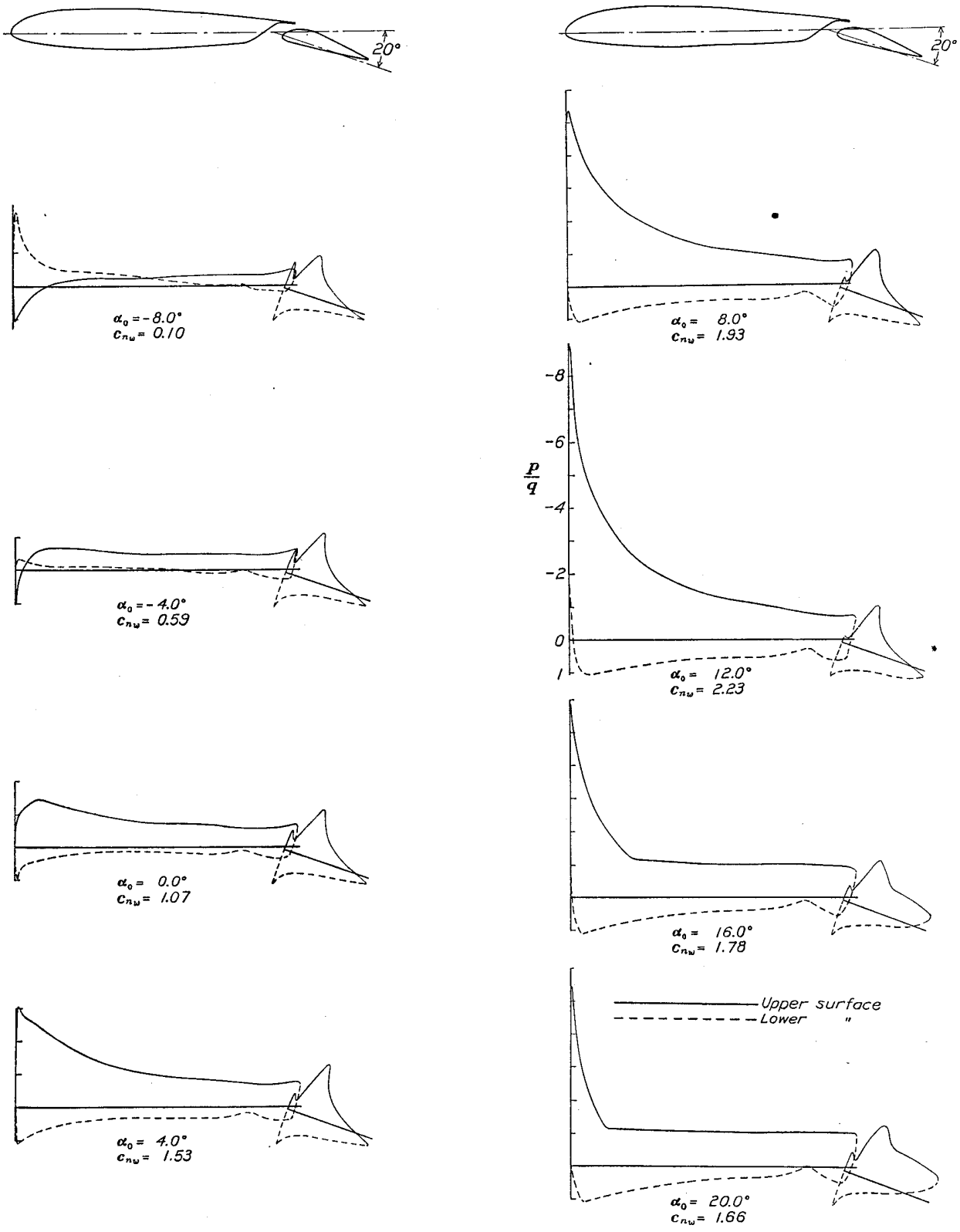

FIGURE 5.—Pressure distribution on the N. A. C. A. 23012 airfoil with a $0.2566c_w$ slotted flap, at various angles of attack. Flap set at 20°.

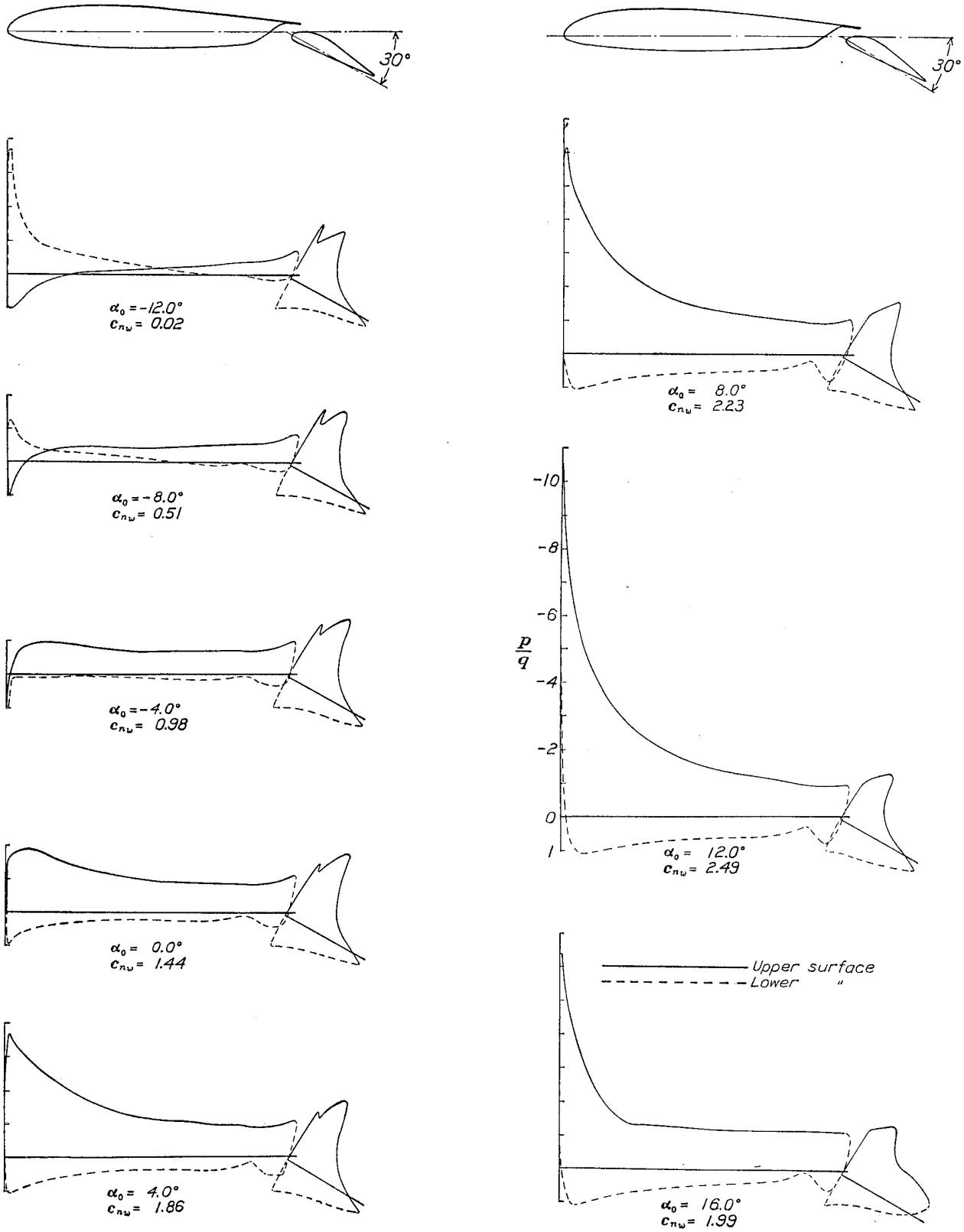

FIGURE 6.—Pressure distribution on the N. A. C. A. 23012 airfoil with a $0.2566c_w$ slotted flap, at various angles of attack. Flap set at 30°

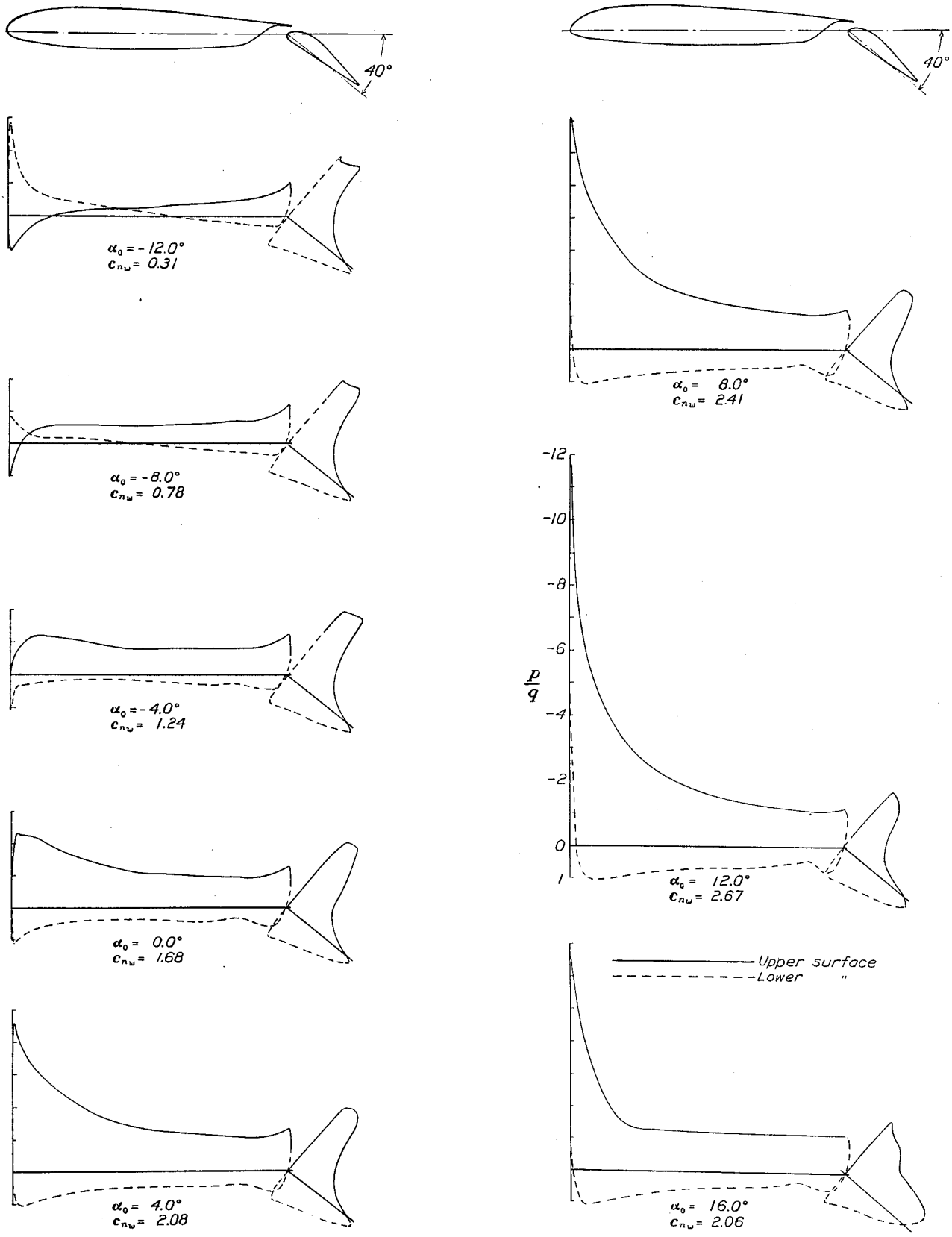

FIGURE 7.—Pressure distribution on the N. A. C. A. 23012 airfoil with a $0.2566c_w$ slotted flap, at various angles of attack. Flap set at 40°.

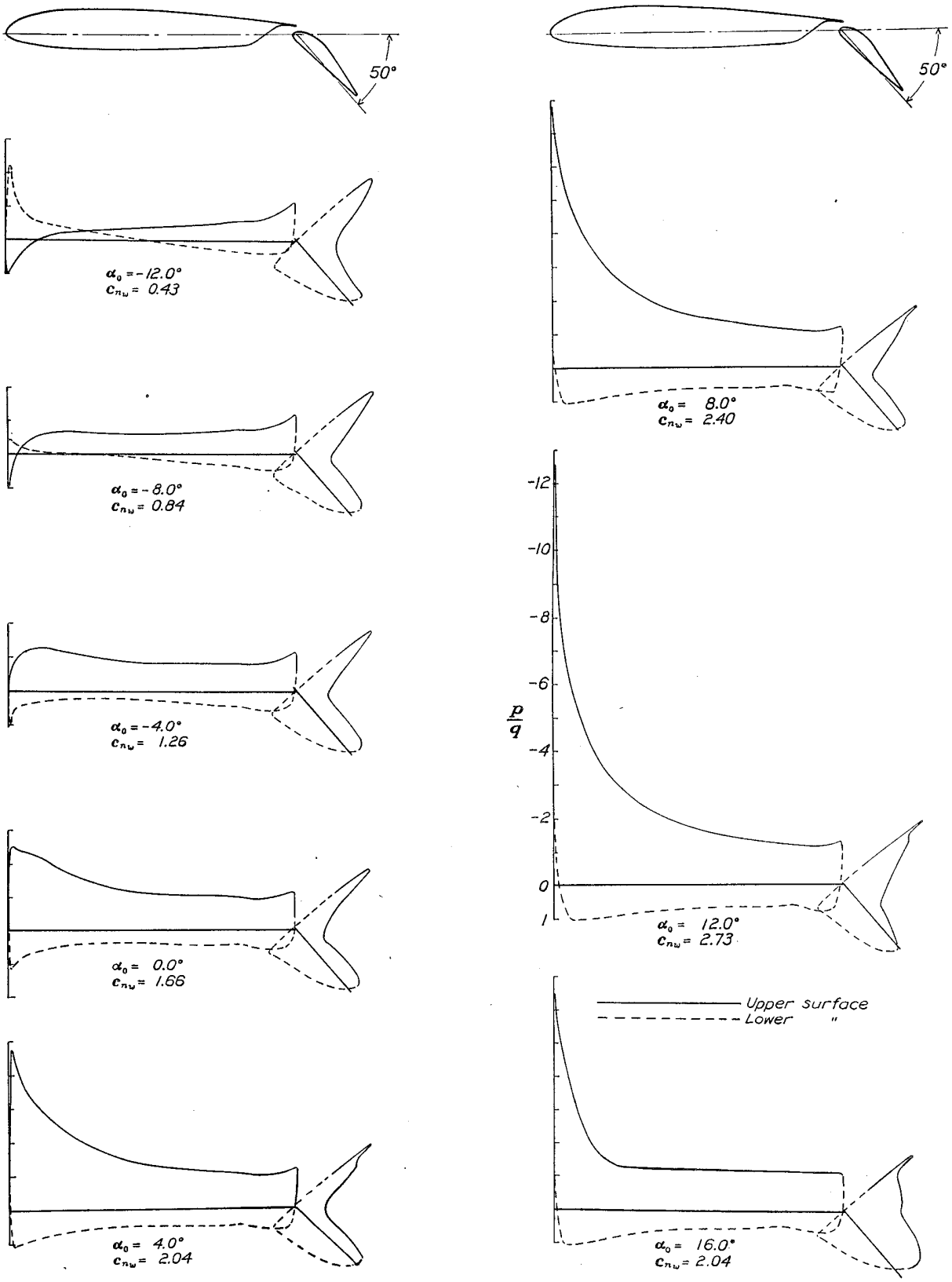

FIGURE 8.—Pressure distribution on the N. A. C. A. 23012 airfoil with a $0.2566c_w$ slotted flap, at various angles of attack. Flap set at 50°.

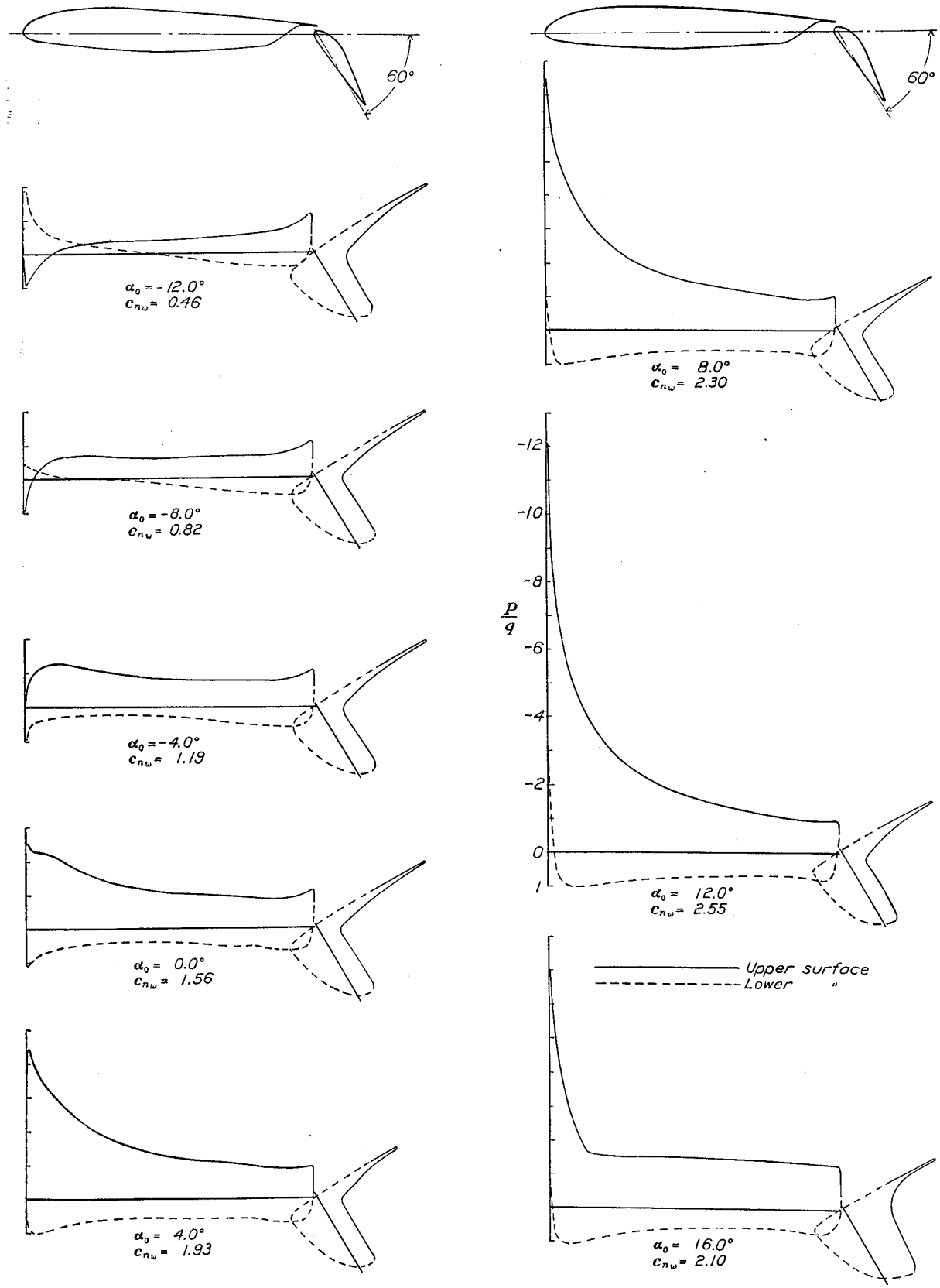

FIGURE 9.—Pressure distribution on the N. A. C. A. 23012 airfoil with a $0.2566c_w$ slotted flap, at various angles of attack. Flap set at 60°.

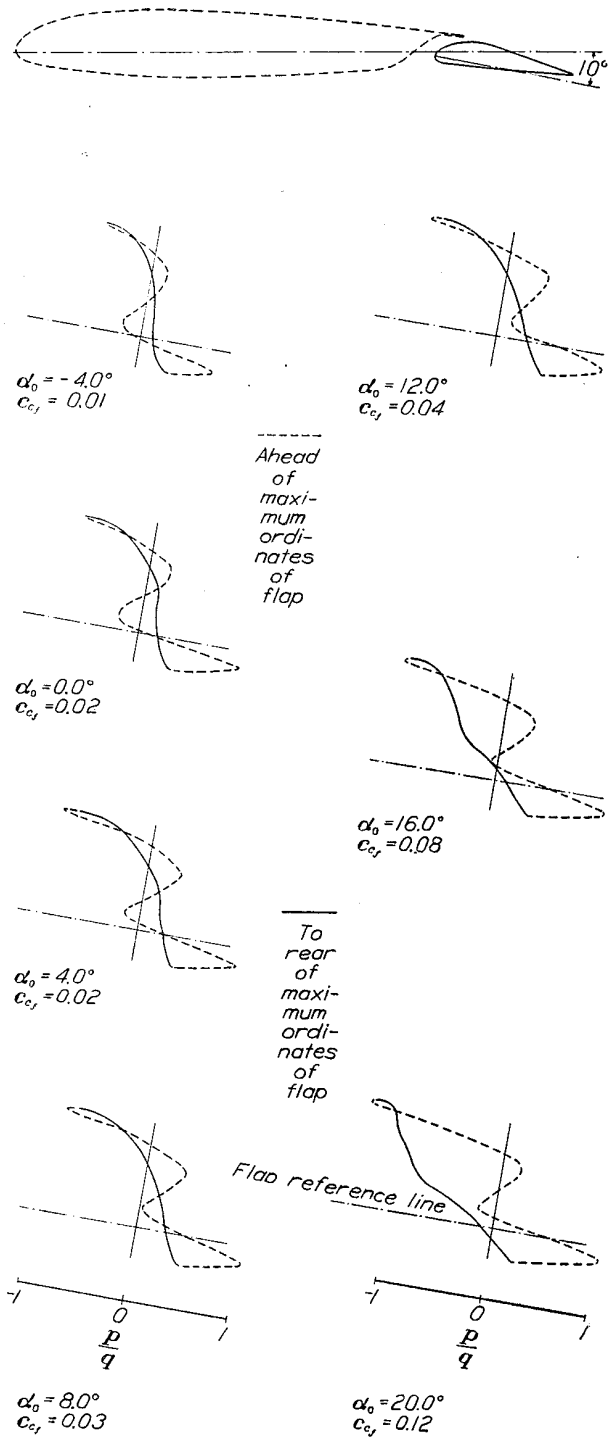

FIGURE 10.—Chord pressure distribution on a $0.2566c_w$ slotted flap mounted on the N. A. C. A. 23012 airfoil. Flap set at 10°.

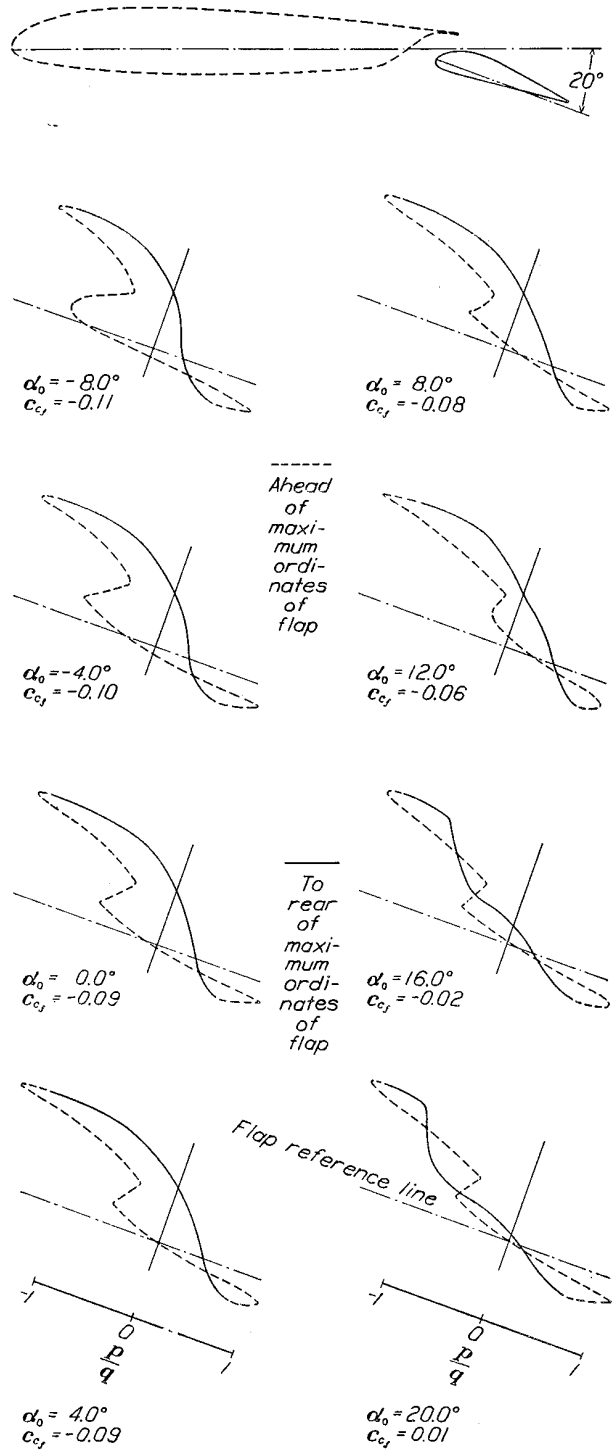

FIGURE 11.—Chord pressure distribution on a $0.2566c_w$ slotted flap mounted on the N. A. C. A. 23012 airfoil. Flap set at 20°.

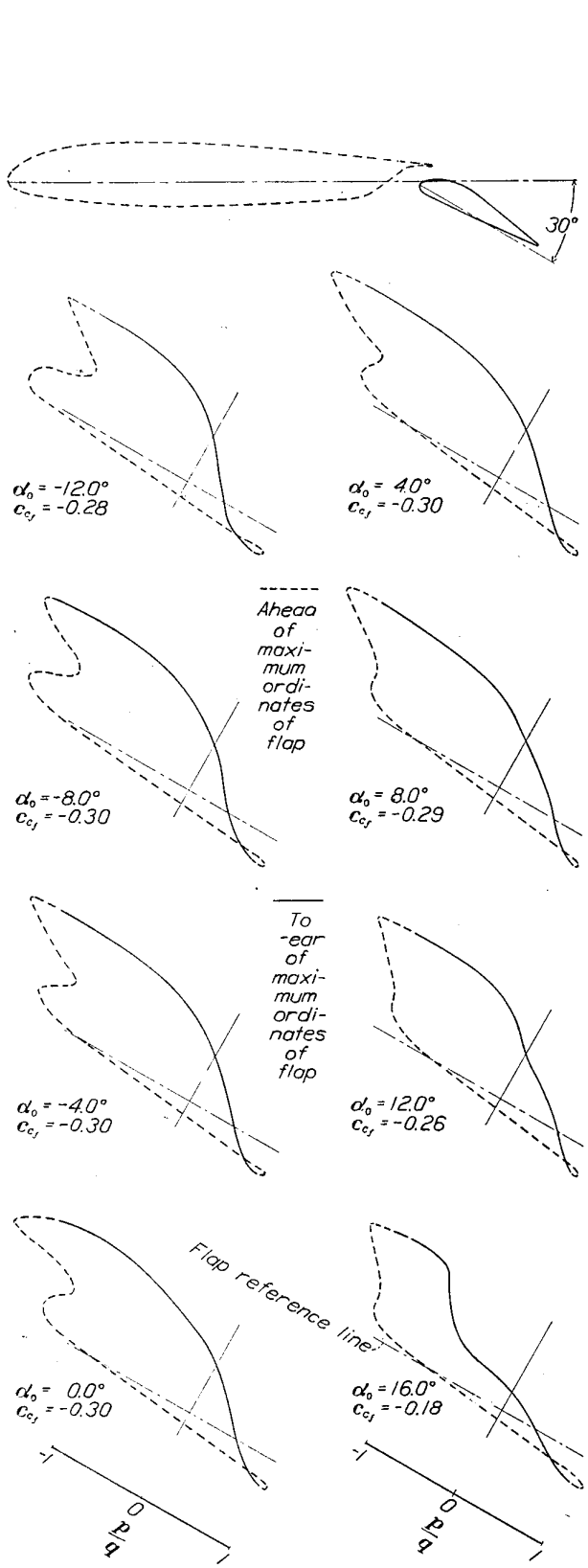

FIGURE 12.—Chord pressure distribution on a $0.2566c_w$ slotted flap mounted on the N. A. C. A. 23012 airfoil. Flap set at 30°.

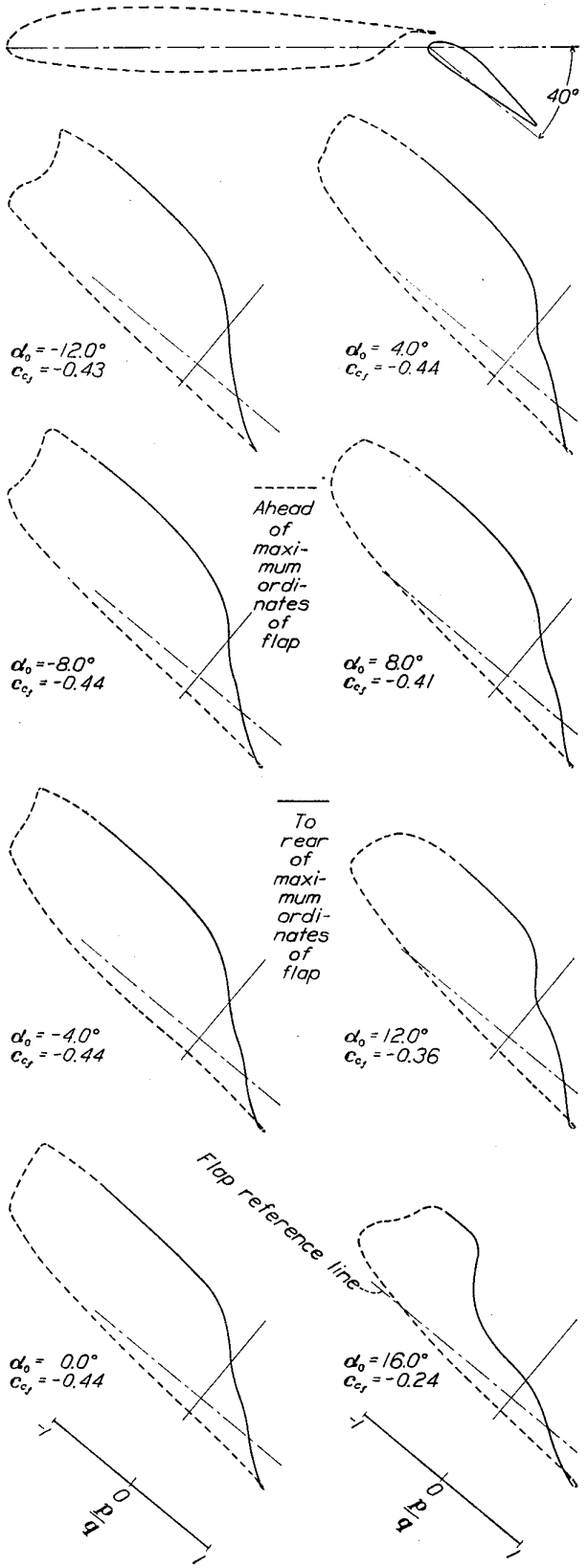

FIGURE 13.—Chord pressure distribution on a $0.2566c_w$ slotted flap mounted on the N. A. C. A. 23012 airfoil. Flap set at 40°.

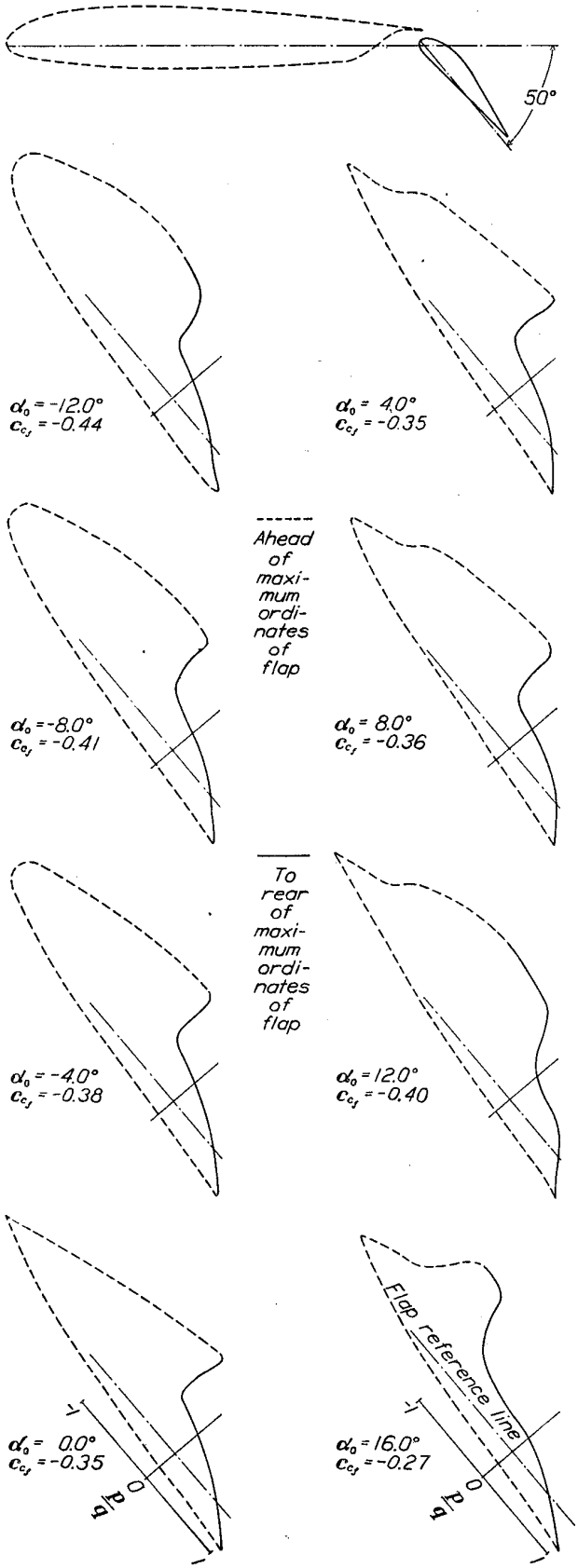

FIGURE 14.—Chord pressure distribution on a $0.2566c_w$ slotted flap mounted on the N. A. C. A. 23012 airfoil. Flap set at 50°.

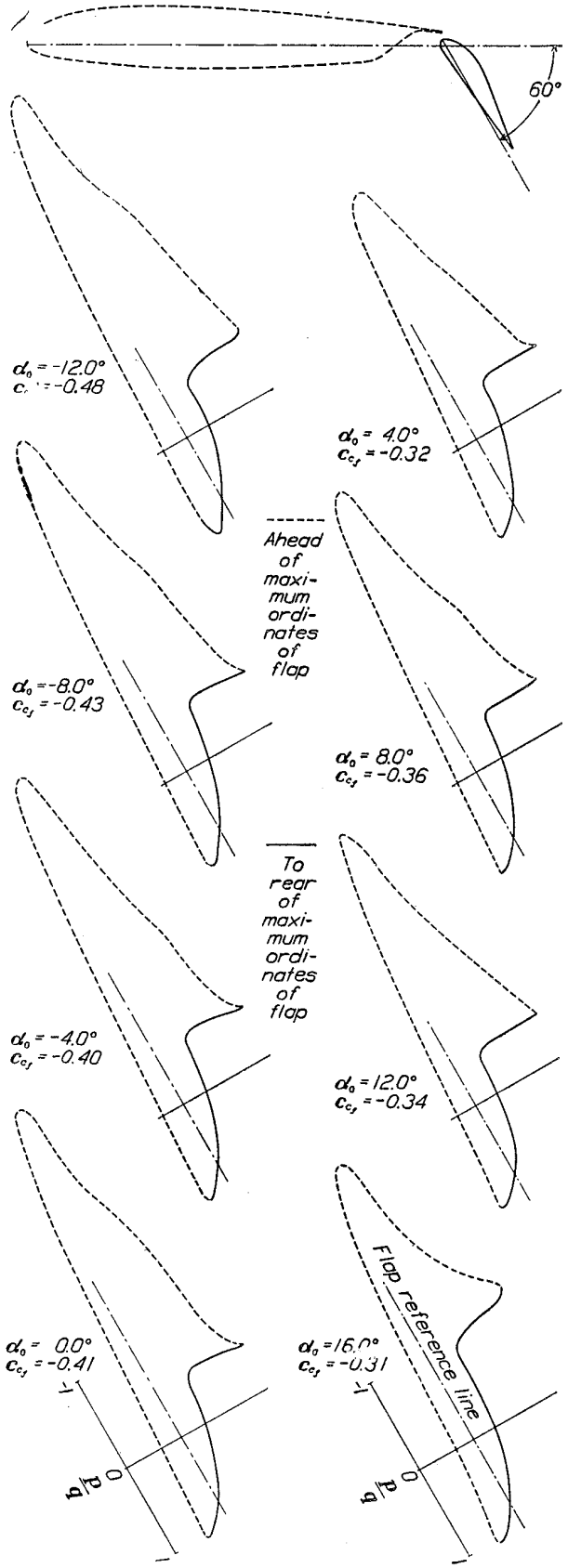

FIGURE 15.—Chord pressure distribution on a $0.2566c_w$ slotted flap mounted on the N. A. C. A. 23012 airfoil. Flap set at 60°.

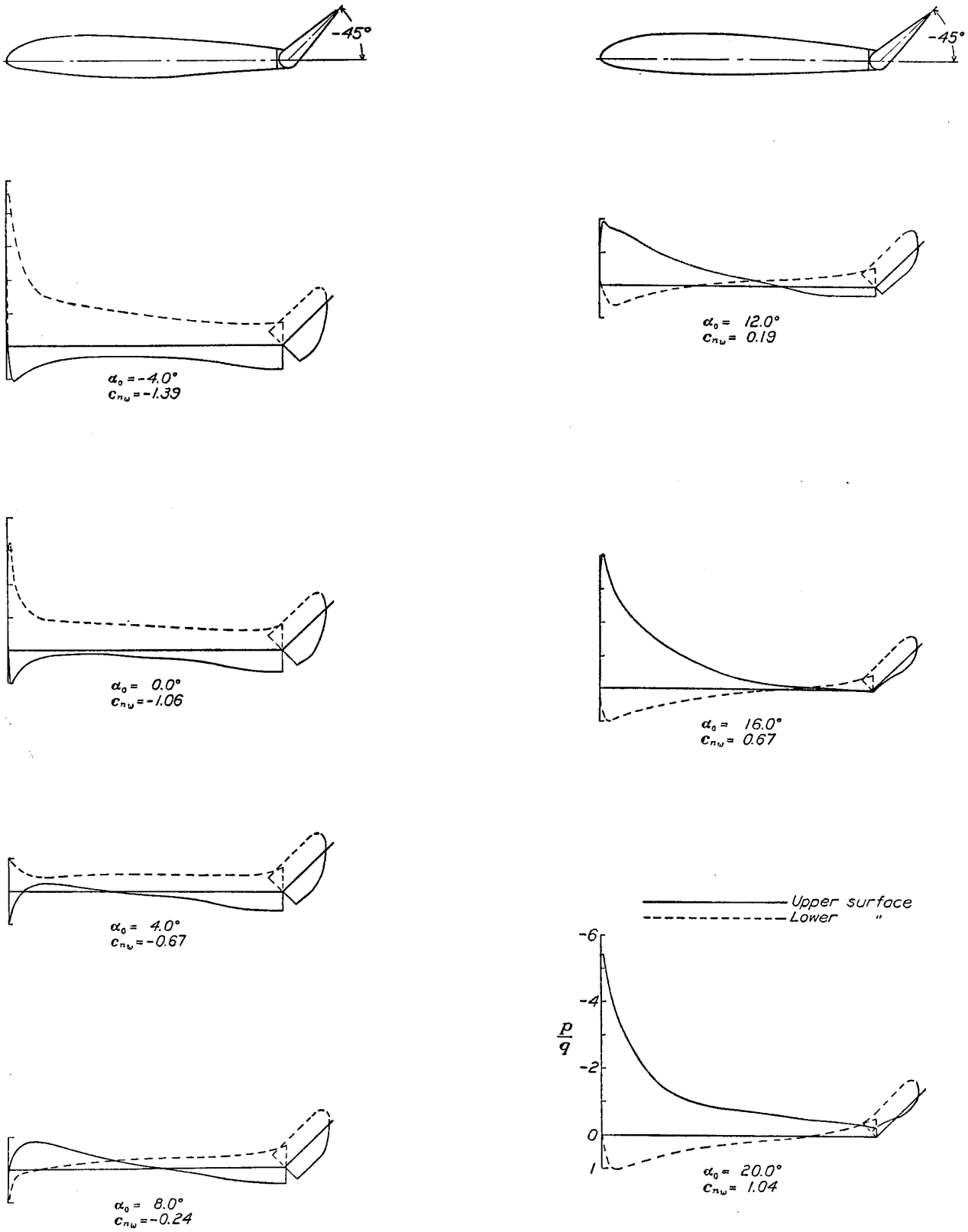

FIGURE 16.—Pressure distribution on the N. A. C. A. 23012 airfoil with a $0.20c_w$ plain flap, at various angles of attack. Flap set at −45°.

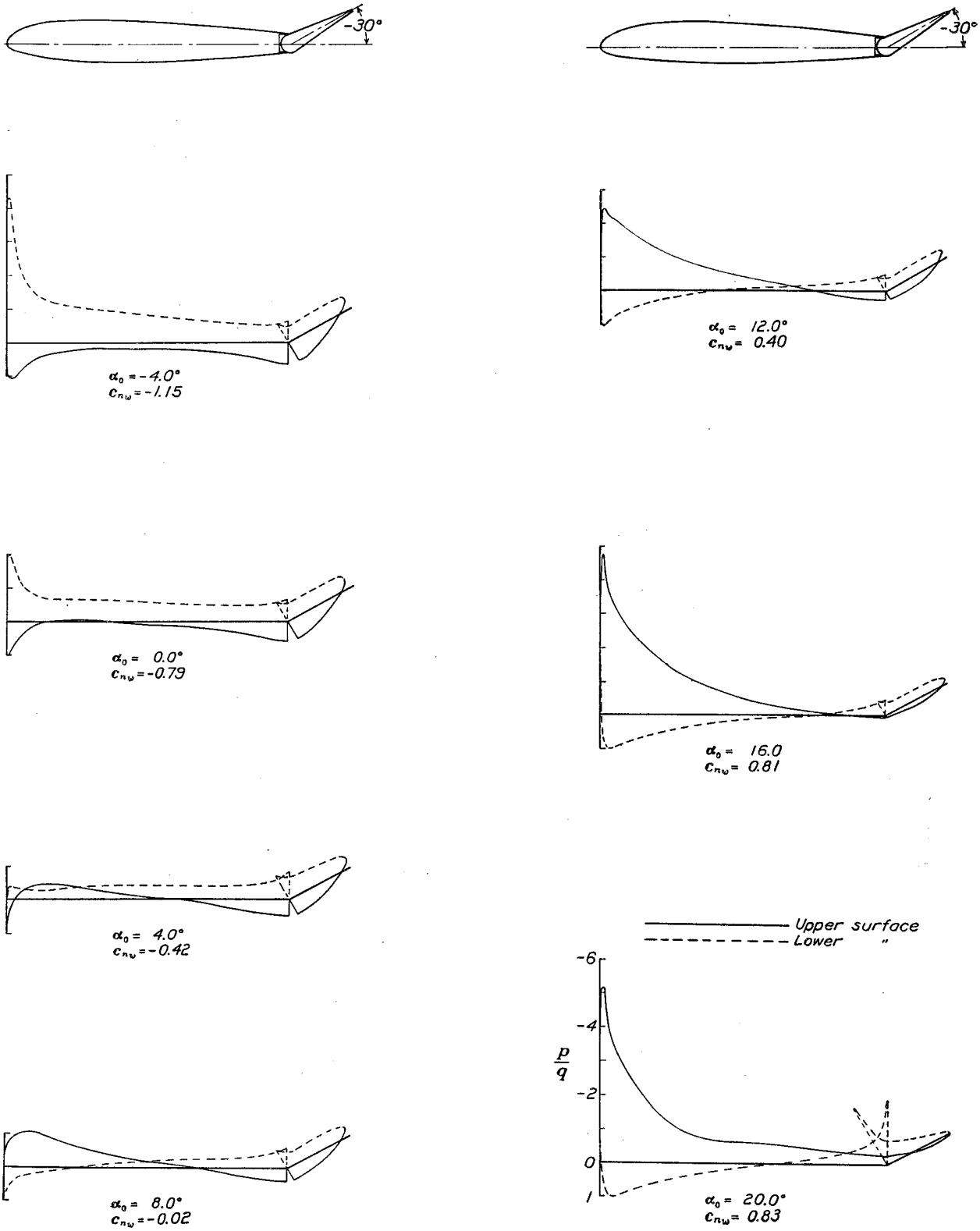

FIGURE 17.—Pressure distribution on the N. A. C. A. 23012 airfoil with a $0.20c_w$ plain flap, at various angles of attack. Flap set at −30°

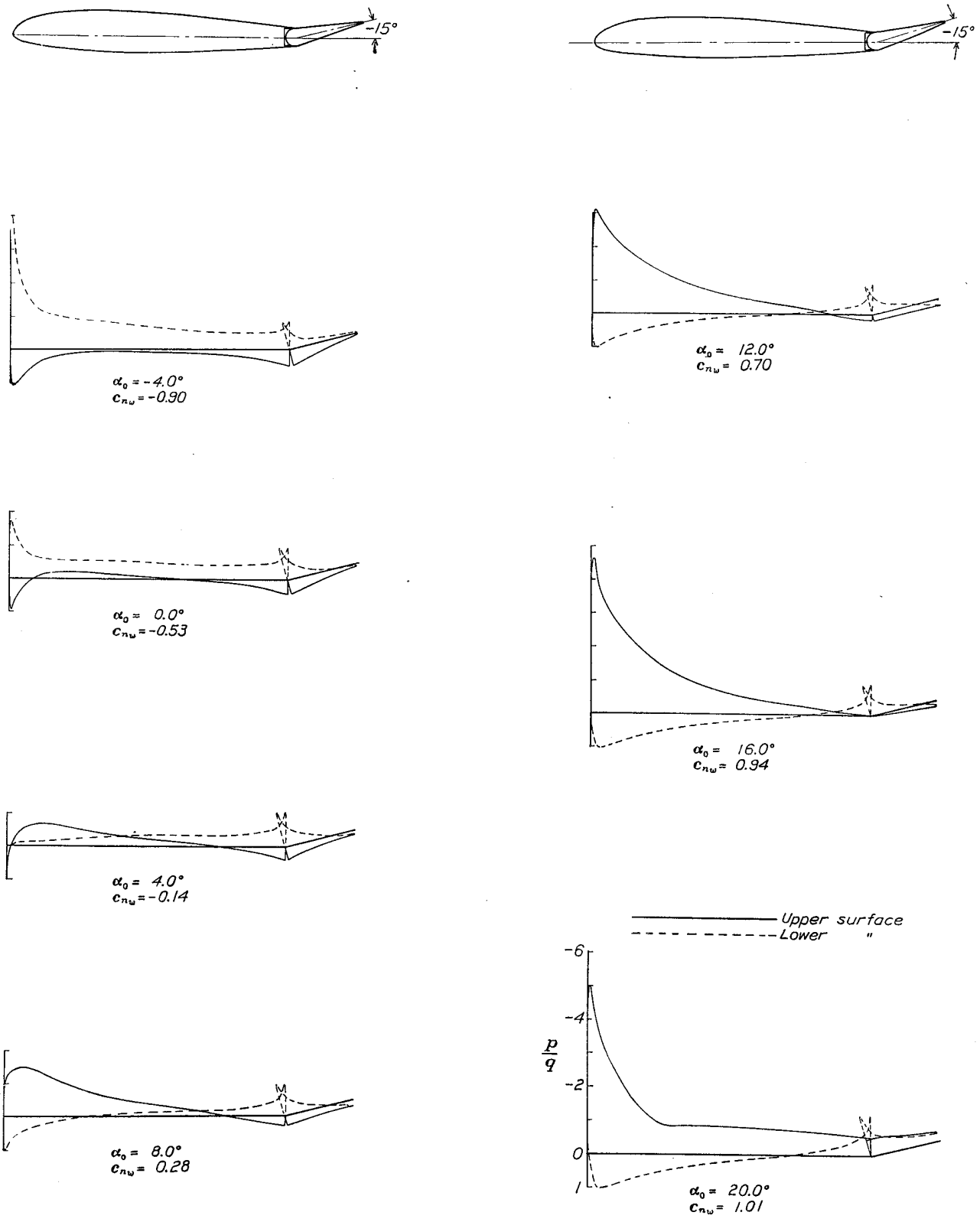

FIGURE 18.—Pressure distribution on the N. A. C. A. 23012 airfoil with a $0.20c_w$ plain flap, at various angles of attack. Flap set at −15°.

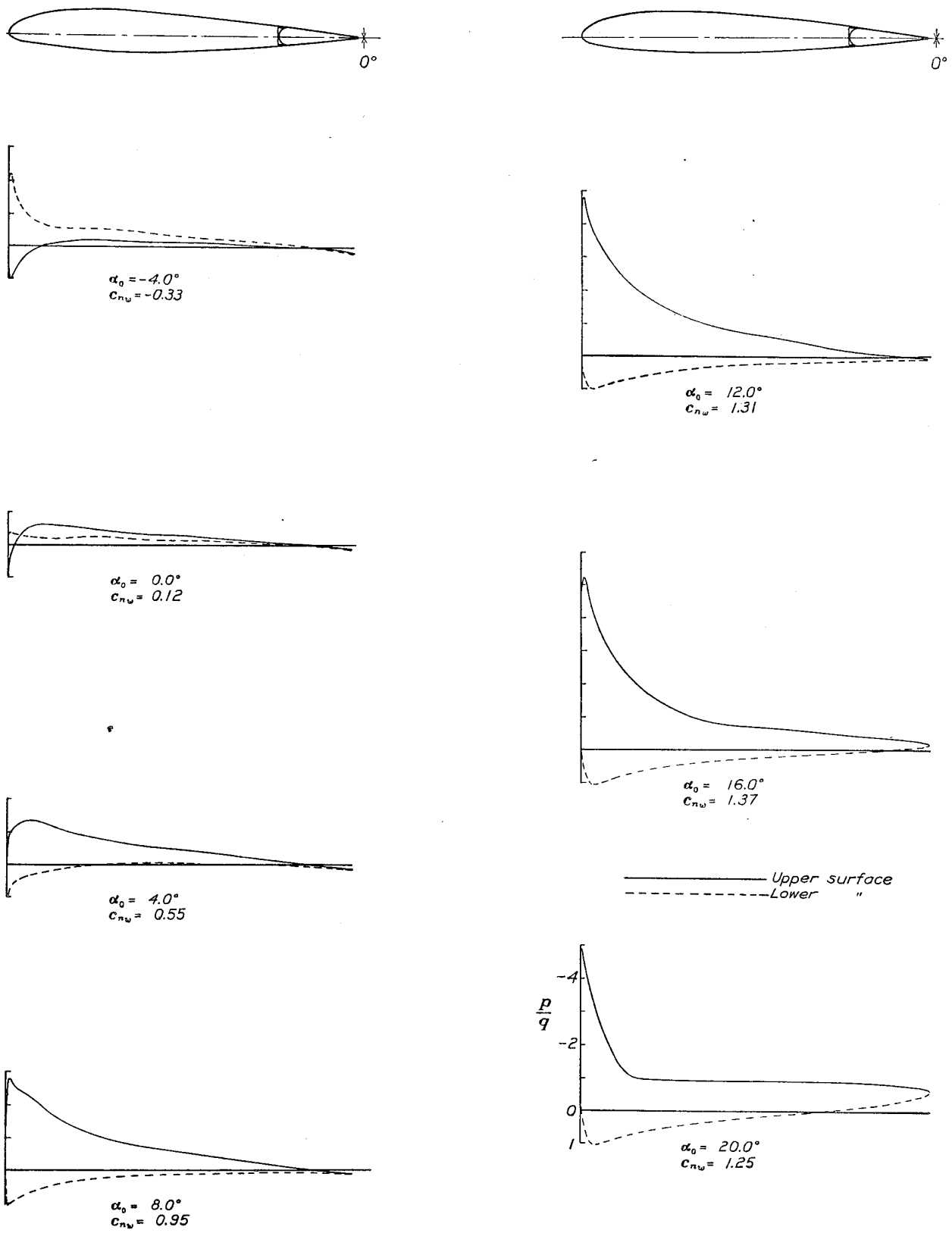

FIGURE 19.—Pressure distribution on the N. A. C. A. 23012 airfoil with a $0.20c_w$ plain flap, at various angles of attack. Flap set at 0°.

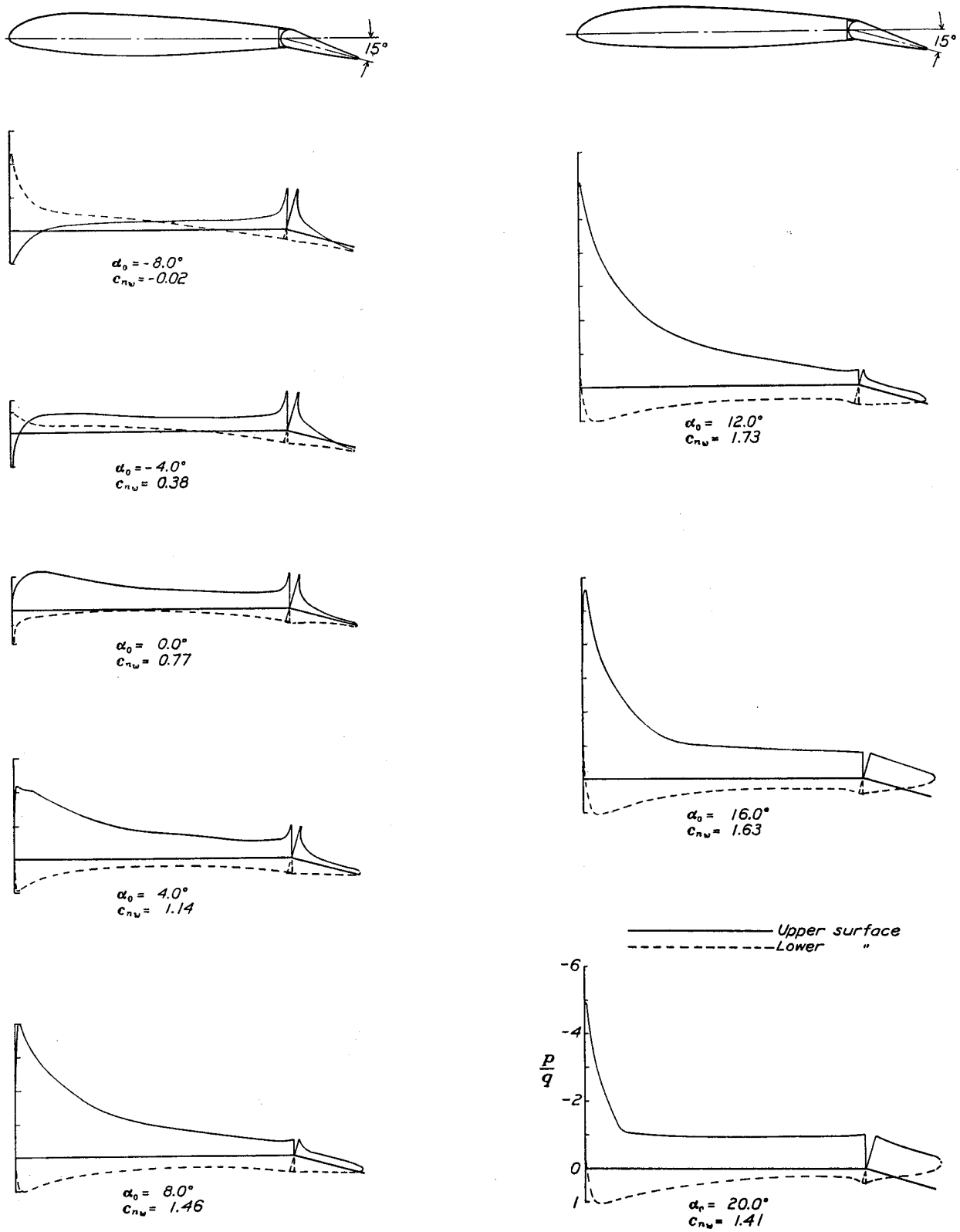

FIGURE 20.—Pressure distribution on the N. A C. A. 23012 airfoil with a $0.20c_w$ plain flap, at various angles of attack. Flap set at 15°.

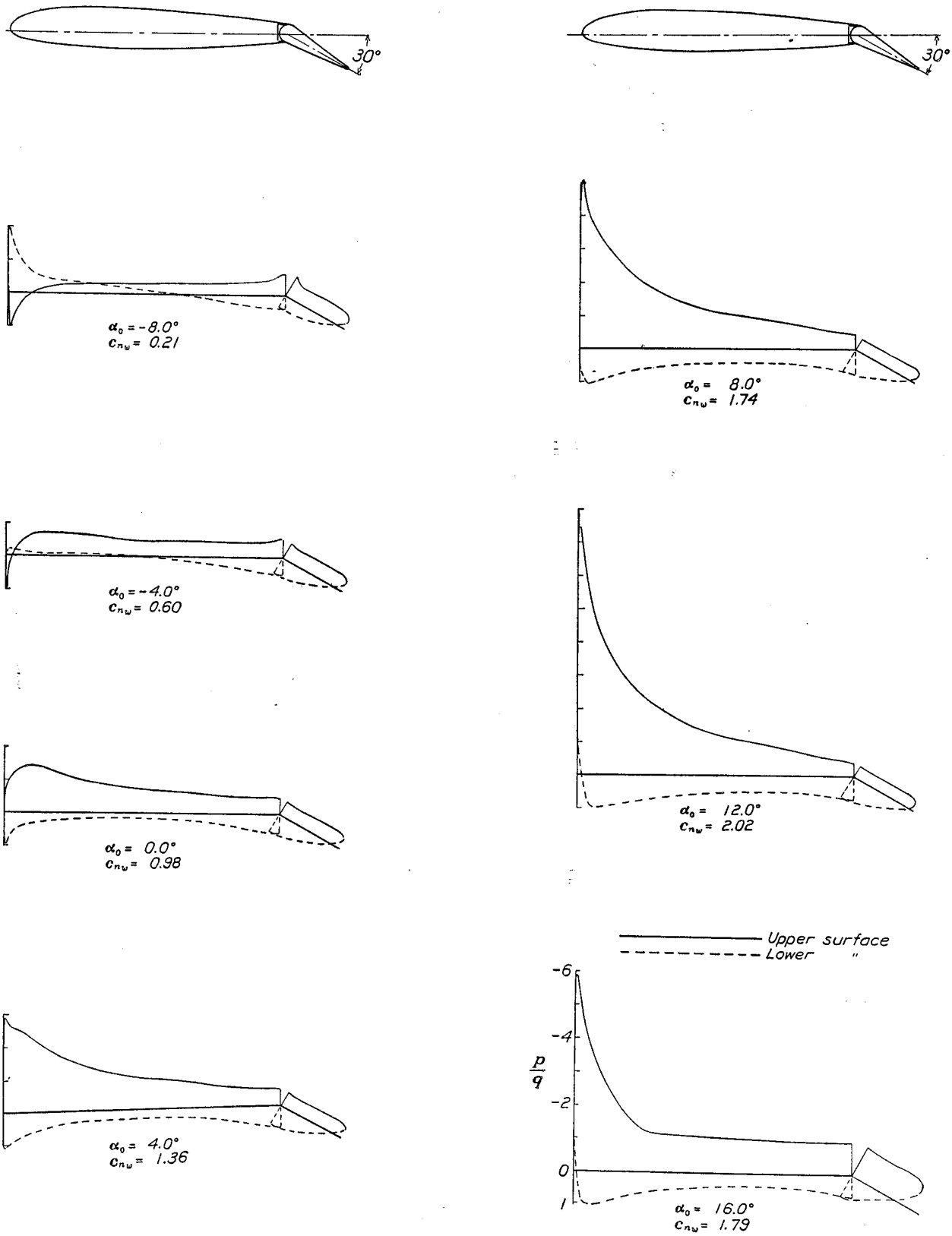

FIGURE 21.—Pressure distribution on the N. A. C. A. 23012 airfoil with a $0.20c_w$ plain flap, at various angles of attack. Flap set at 30°.

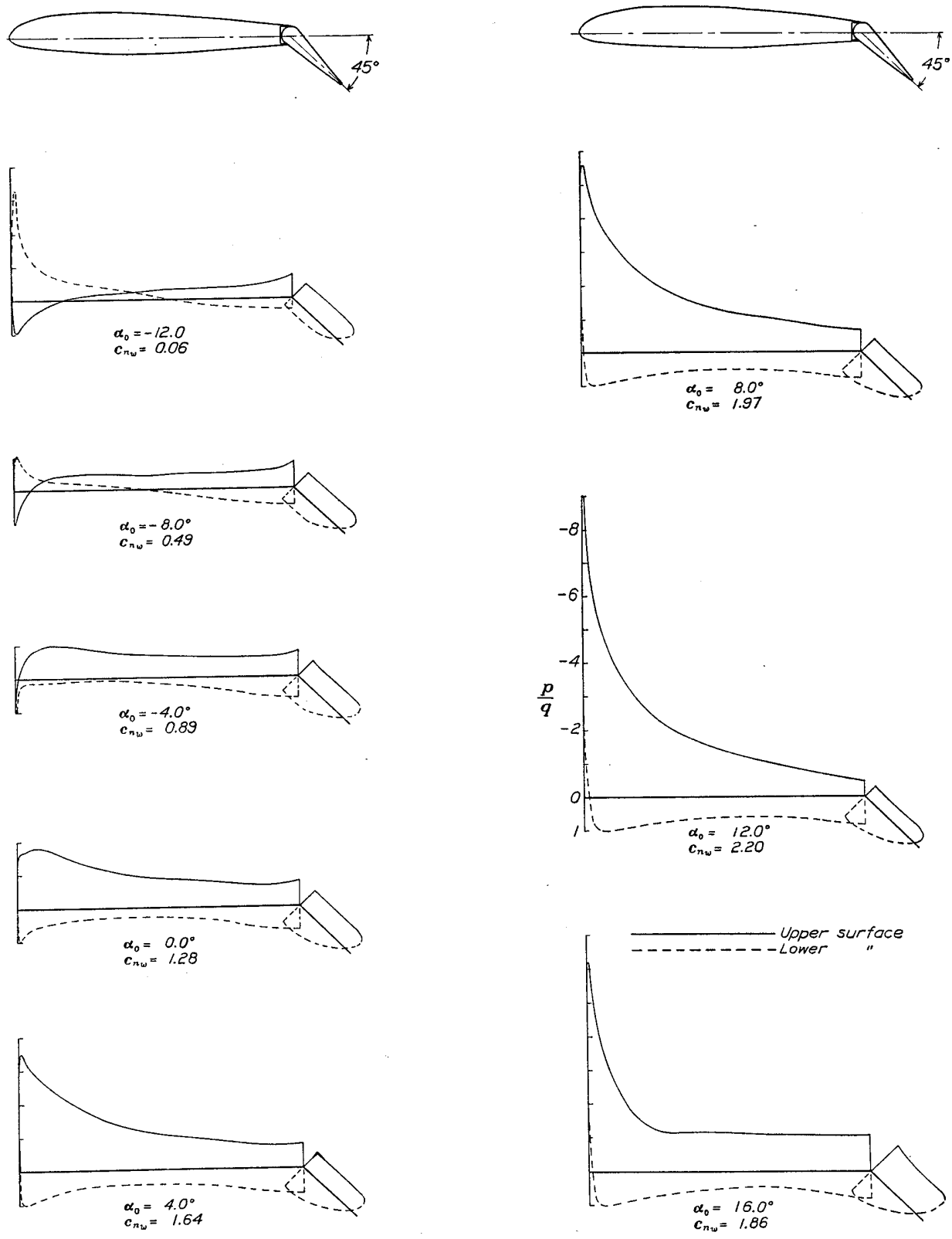

FIGURE 22.—Pressure distribution on the N. A. C. A. 23012 airfoil with a $0.20c_w$ plain flap, at various angles of attack. Flap set at 45°.

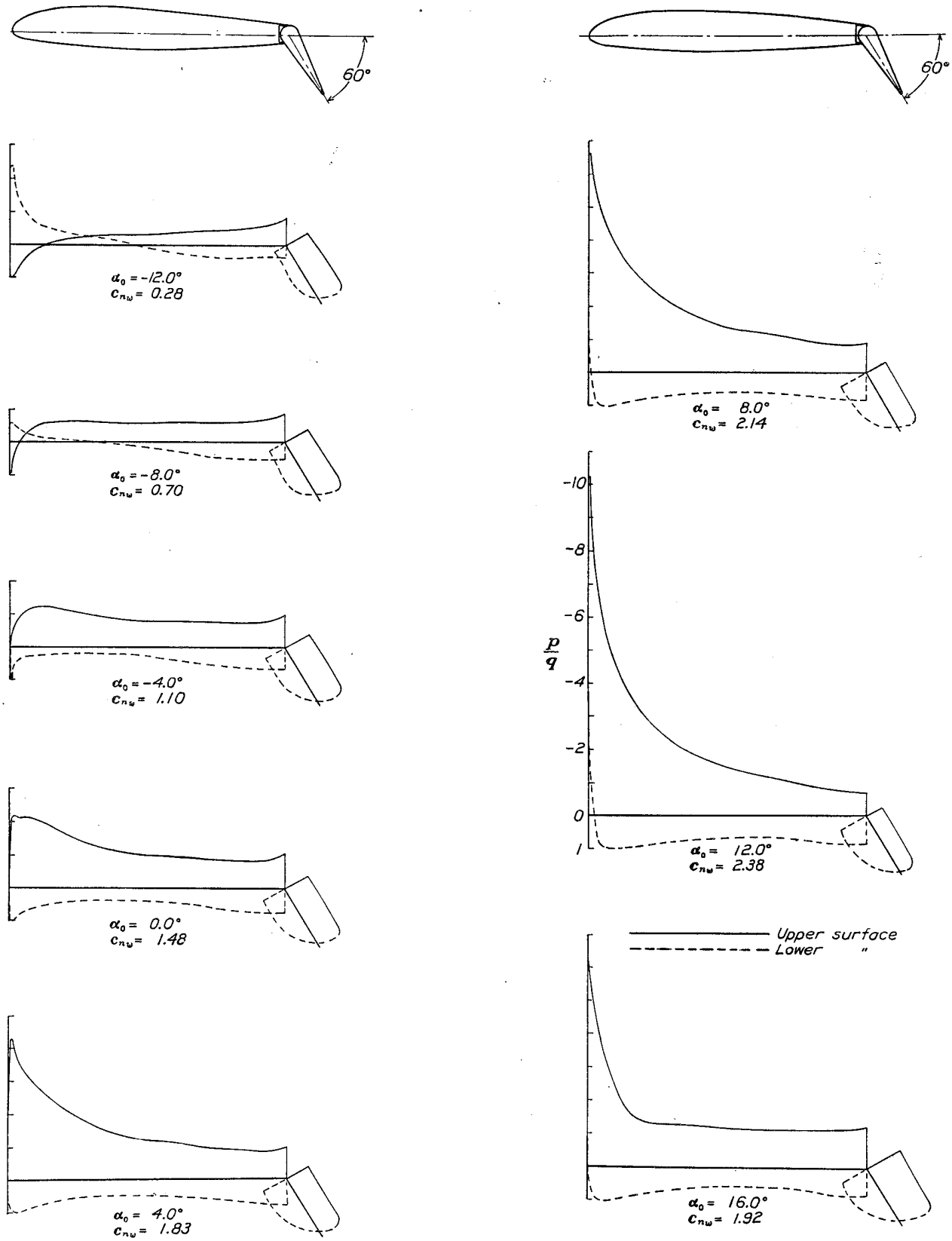

FIGURE 23.—Pressure distribution on the N. A. C. A. 23012 airfoil with a $0.20c_w$ plain flap, at various angles of attack. Flap set at 60°.

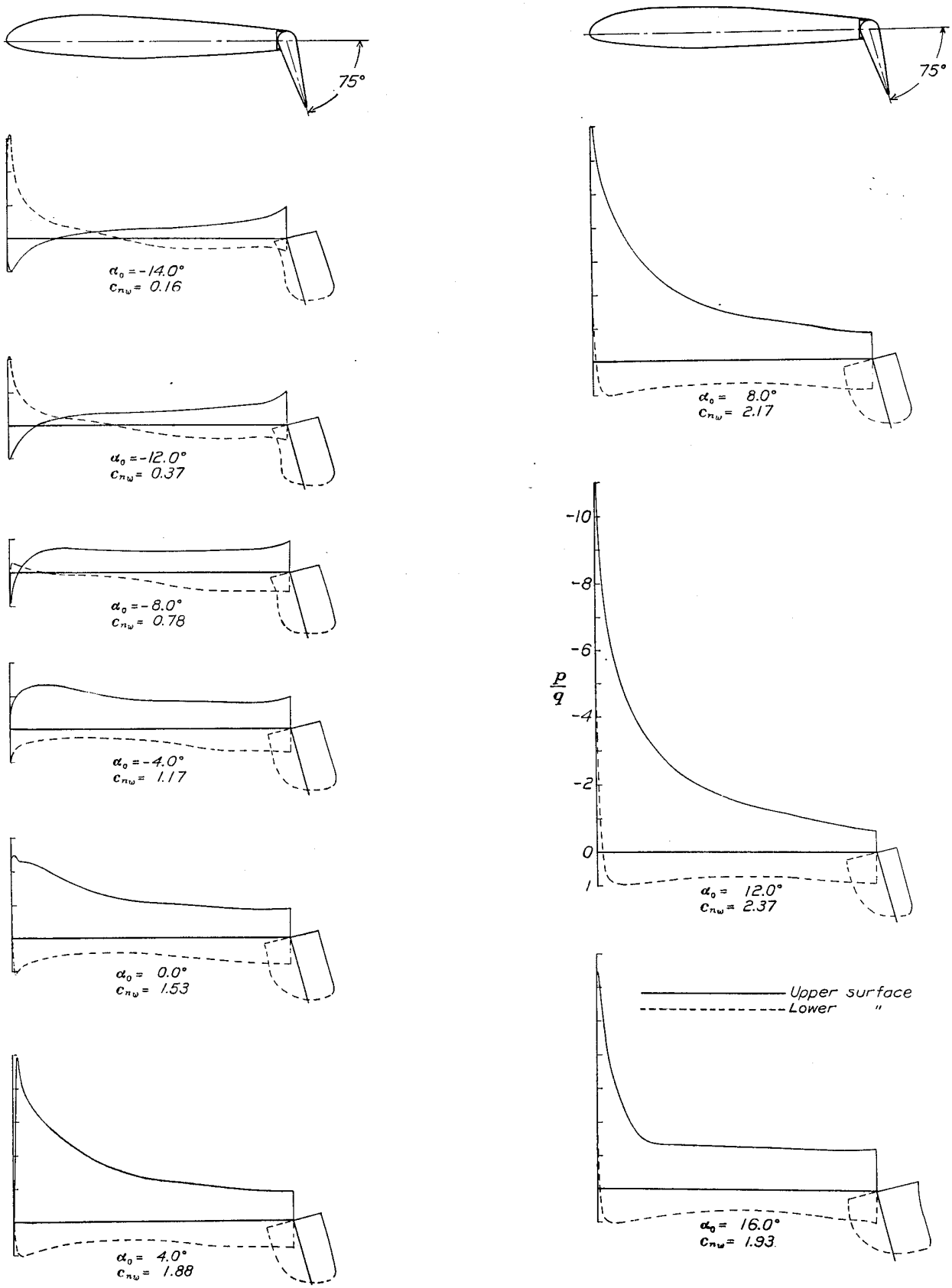

FIGURE 24.—Pressure distribution on the N. A. C. A. 23012 airfoil with a $0.20c_w$ plain flap, at various angles of attack. Flap set at 75°.

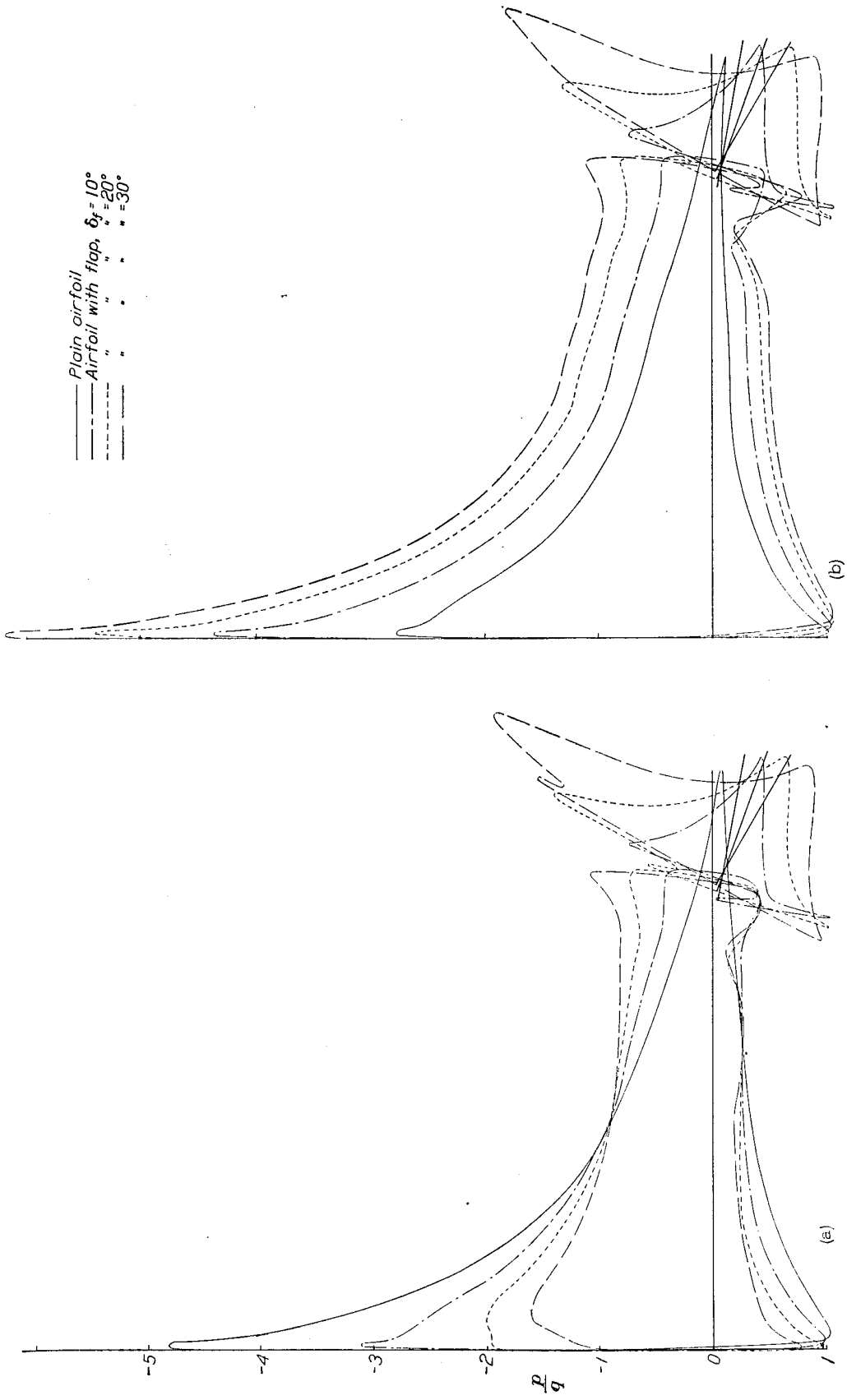

(a) At the same lift, $c_{n_w} = 1.31$.

(b) At the same angle of attack, $\alpha_0 = 8°$.

FIGURE 25.—Comparison of the pressure distribution on an N. A. C. A. 23012 airfoil and a 0.2566c_w slotted flap with that on the plain airfoil.

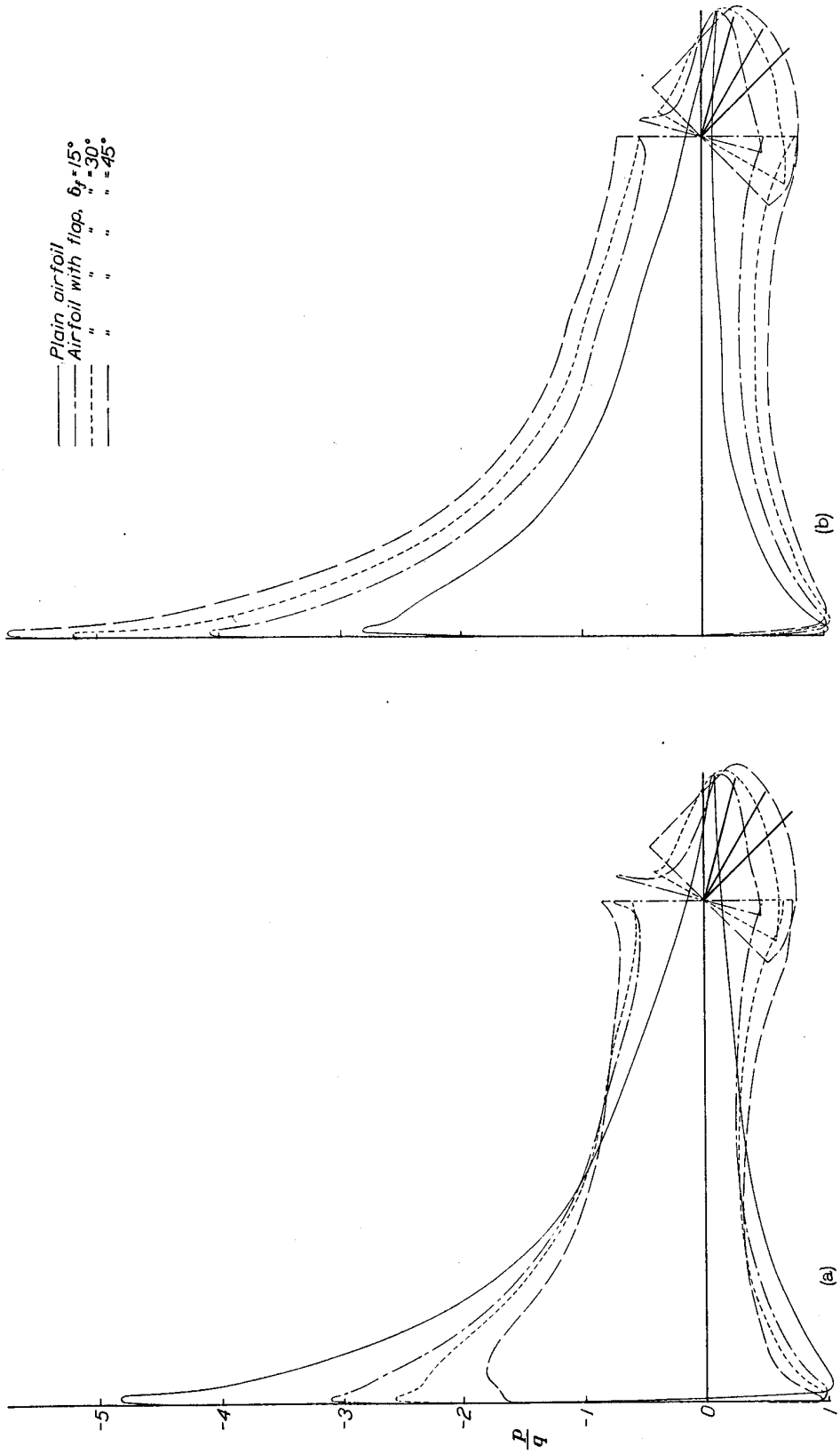

(b) At the same angle of attack, $\alpha_a = 8°$.

(a) At the same lift, $c_{n,a} = 1.31$.

FIGURE 26.—Comparison of the pressure distribution on an N. A. C. A. 23012 airfoil and a $0.20c_a$ plain flap with that on the plain airfoil.

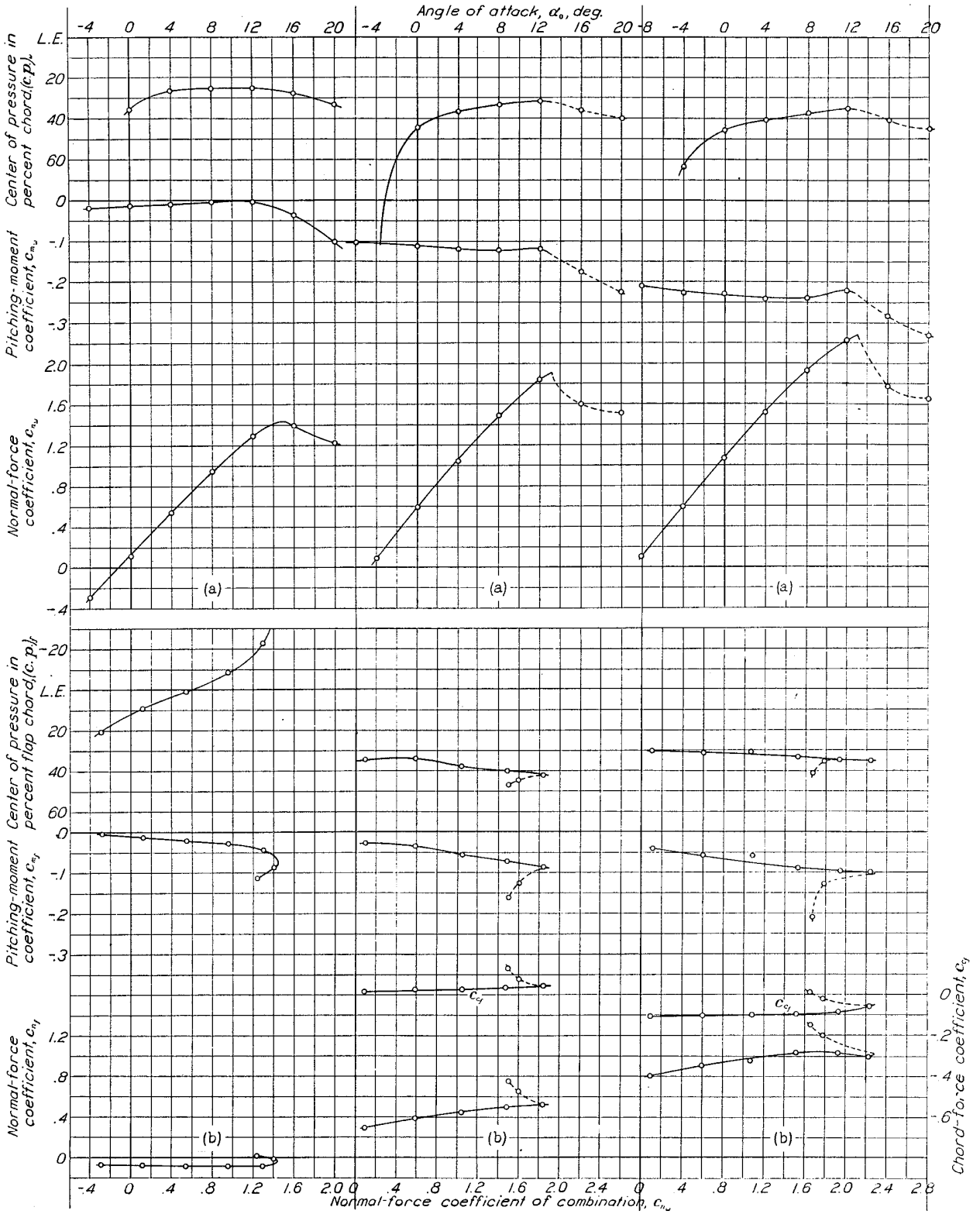

(a) Airfoil with flap.
(b) Flap alone.

FIGURE 27.—Section characteristics of the N. A. C. A. 23012 airfoil with a $0.2566c_w$ slotted flap set at 0°.

(a) Airfoil with flap.
(b) Flap alone.

FIGURE 28.—Section characteristics of the N. A. C. A. 23012 airfoil with a $0.2566c_w$ slotted flap set at 10°

(a) Airfoil with flap.
(b) Flap alone.

FIGURE 29.—Section characteristics of the N. A. C. A. 23012 airfoil with a $0.2566c_w$ slotted flap set at 20°.

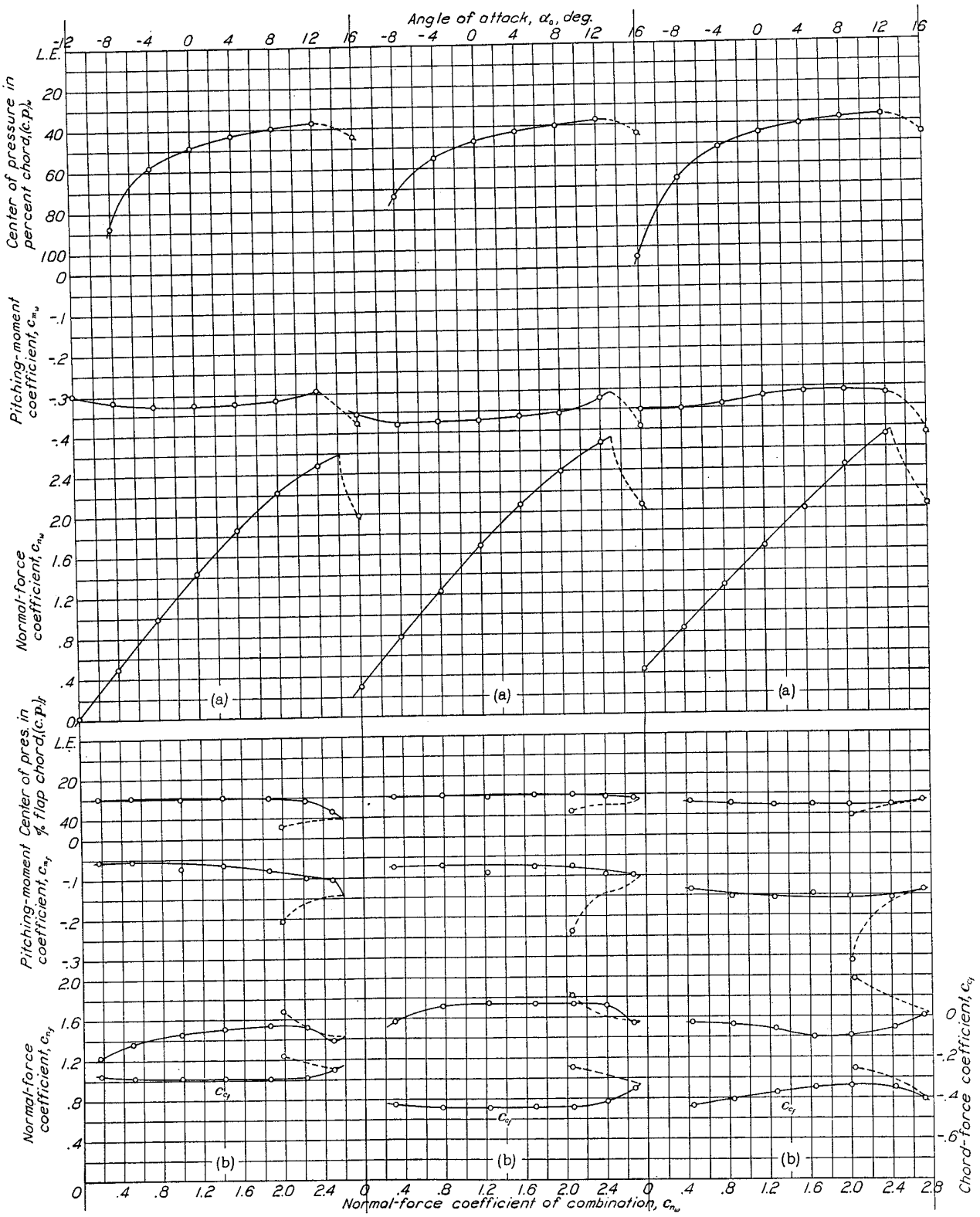

(a) Airfoil with flap.
(b) Flap alone.

FIGURE 30.—Section characteristics of the N. A. C. A. 23012 airfoil with a $0.2566c_w$ slotted flap set at 30°.

(a) Airfoil with flap.
(b) Flap alone.

FIGURE 31.—Section characteristics of the N. A. C. A. 23012 airfoil with a $0.2566c_w$ slotted flap set at 40°.

(a) Airfoil with flap.
(b) Flap alone.

FIGURE 32.—Section characteristics of the N. A. C. A. 23012 airfoil with a $0.2566c_w$ slotted flap set at 50°.

pressures near the leading edges, which, at high angles of attack, checked to within ±5 percent. The dynamic pressure recorded was accurate to within ±0.25 percent for all tests. Pressure orifices were not sufficiently numerous to determine accurately the peaks of pressures on the airfoil nose, but this deficiency should not materially affect the results.

RESULTS AND DISCUSSION

SECTION PRESSURE DISTRIBUTION

The distributions of air loads on the main airfoil and on the two types of flap are shown in figures 3 to 26. These pressure diagrams may be applied to the structural design of ribs and flaps and, in addition, figures 16 to 24 are useful in that they supply considerable detailed information for the structural design of plain ailerons. The pressure diagrams also serve to illustrate some important effects of the action of flaps on the distribution of pressures over the airfoil.

A comparison of the pressures over the upper surface of the slotted flap (figs. 3 to 9) with those of the plain flap (figs. 16 to 24), or with those of either the external-airfoil flap (reference 5) or some Fowler flaps (reference 6), indicates certain differences, the most obvious of which is a double-peak negative pressure region near the nose. These peaks may be interpreted as indicating the existence of relatively high-velocity regions with a low-velocity region between them.

An analysis of figures 4 to 7 shows that this region of decreased velocity, or increased pressure, moved forward on the flap as the flap deflection was increased. For flap deflections of 10°, 20°, 30°, and 40° this region was located at approximately 2, 1½, 1, and ½ percent of the main airfoil chord, respectively, behind the leading edge of the flap. Because of its path, the nose of the flap moved back correspondingly greater increments when the flap was deflected; therefore the resultant movement of the region of decreased velocity was backward toward the edge of the lip as the flap deflection was increased. The double-peak pressures finally disappeared at high angles of attack for a flap deflection of 30° (fig. 6) and at low angles of attack for a flap deflection of 40° (fig. 7). As the angle of attack was increased for a given flap deflection (figs. 4 to 7), the double-peak pressure distribution slowly approached a single-peak pressure distribution. It is interesting to note that these peak negative pressures on the slotted flap extended over a greater portion of the flap chord than did corresponding peak pressures over other flaps (references 5 and 6).

The peak pressures over the upper surface of the slotted flap are not so high as the corresponding peak pressures over an external-airfoil flap, but they are much higher than those over the plain flap (figs. 16 to 24). No data are available, however, for the external-airfoil flap for flap deflections above 40°, but it is believed that the slotted flap would develop higher peak pressures because it can be set at higher flap deflections before completely stalling. The upper surface of

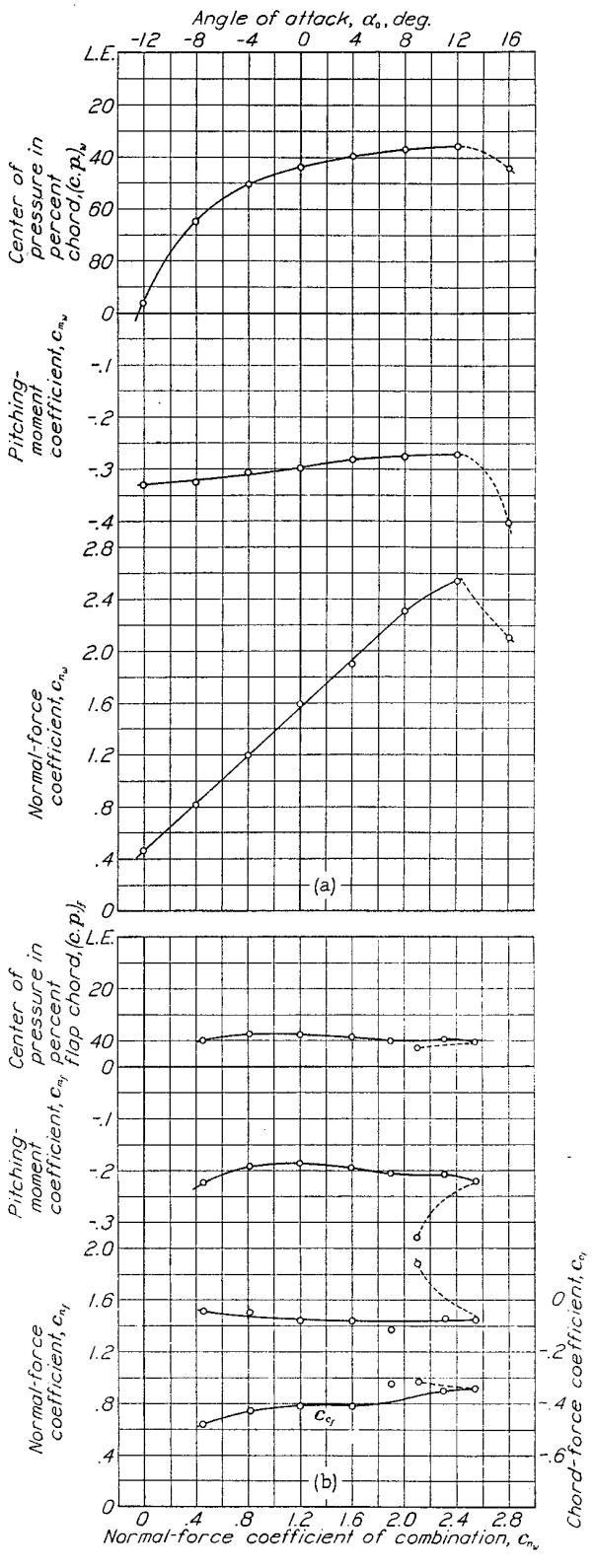

(a) Airfoil with flap.
(b) Flap alone.

FIGURE 33.—Section characteristics of the N. A. C. A. 23012 airfoil with a 0.2566c_w slotted flap set at 60°.

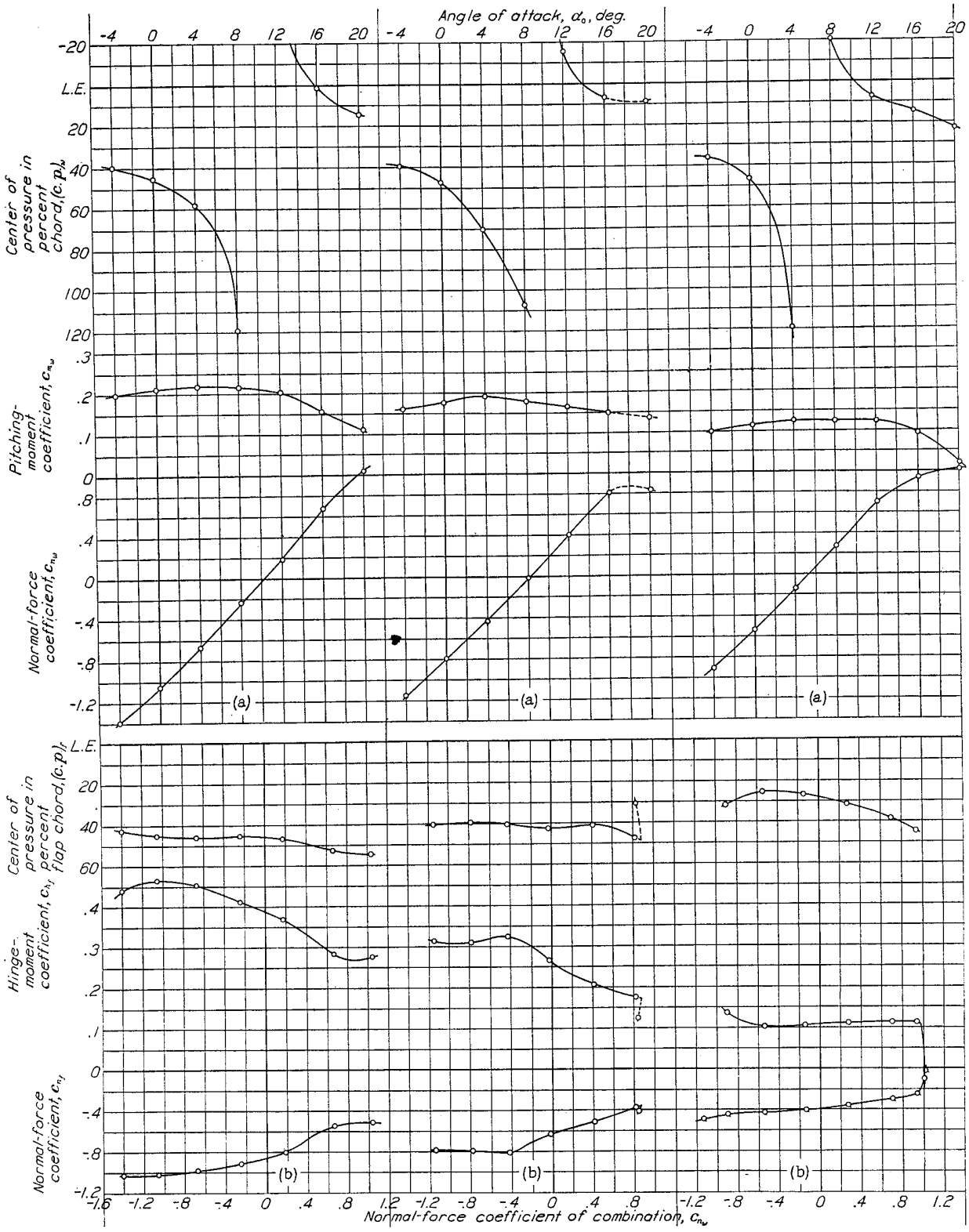

(a) Airfoil with flap.
(b) Flap alone.

FIGURE 34.—Section characteristics of the N. A. C. A. 23012 airfoil with a $0.20c_w$ plain flap set at −45°.

(a) Airfoil with flap.
(b) Flap alone.

FIGURE 35.—Section characteristics of the N. A. C. A. 23012 airfoil with a $0.20c_w$ plain flap set at −30°.

(a) Airfoil with flap.
(b) Flap alone.

FIGURE 36.—Section characteristics of the N. A. C. A. 23012 airfoil with a $0.20c_w$ plain flap set at −15°.

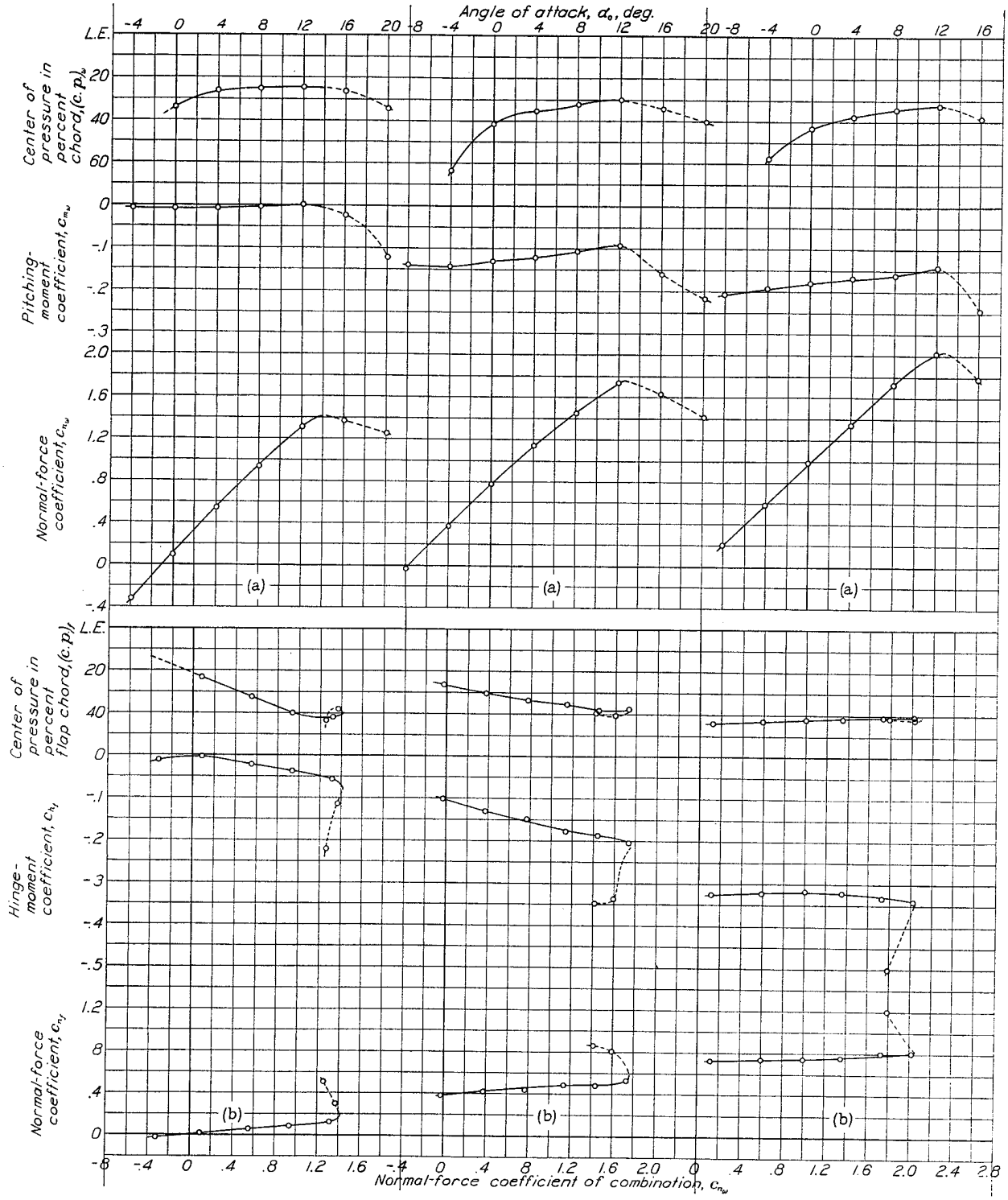

(a) Airfoil with flap.
(b) Flap alone.

FIGURE 37.—Section characteristics of the N. A. C. A. 23012 airfoil with a $0.20c_w$ plain flap set at 0°.

(a) Airfoil with flap.
(b) Flap alone.

FIGURE 38.—Section characteristics of the N. A. C. A. 23012 airfoil with a $0.20c_w$ plain flap set at 15°.

(a) Airfoil with flap.
(b) Flap alone.

FIGURE 39.—Section characteristics of the N. A. C. A. 23012 airfoil with a $0.20c_w$ plain flap set at 30°.

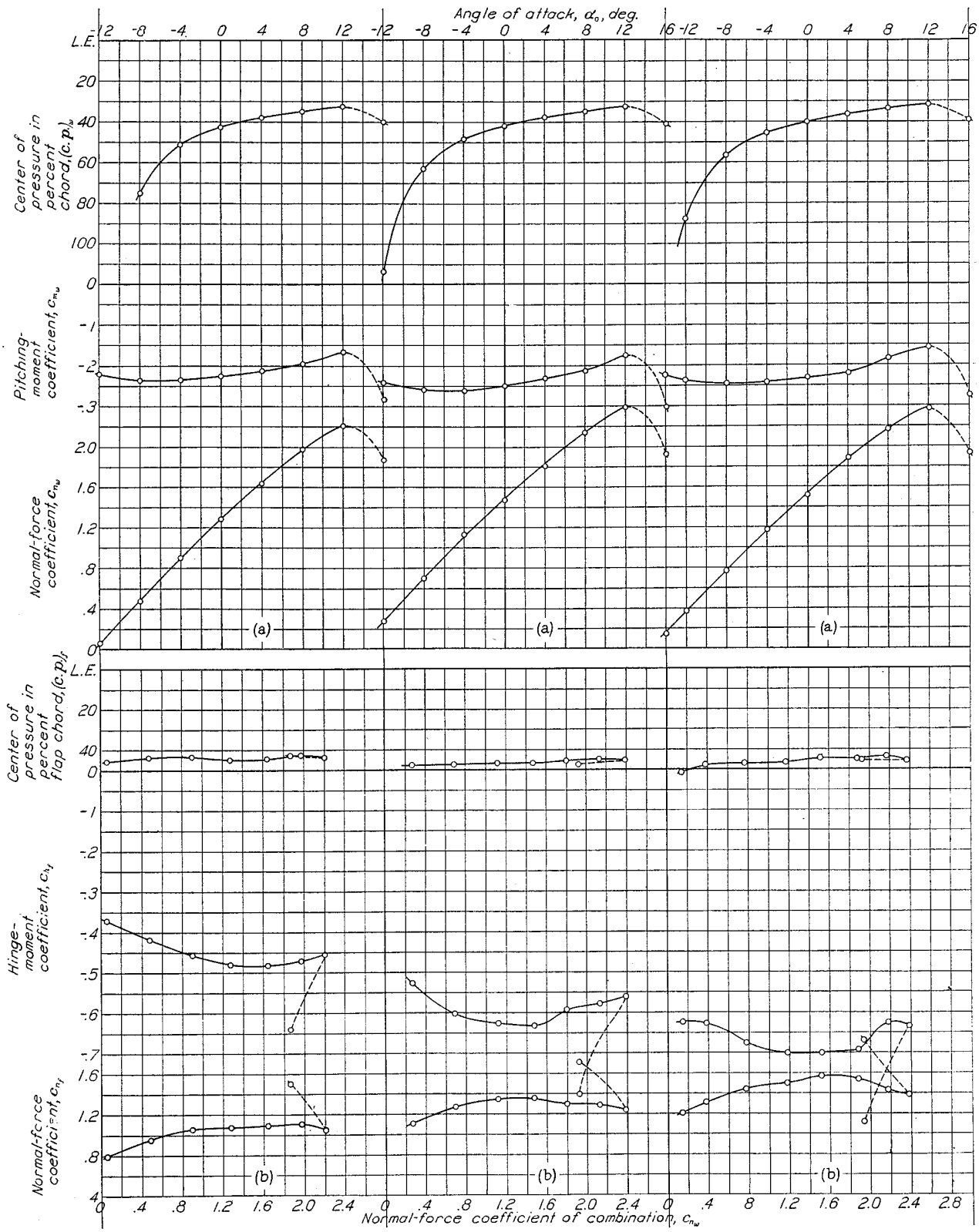

(a) Airfoil with flap.
(b) Flap alone.

FIGURE 40.—Section characteristics of the N. A. C. A. 23012 airfoil with a $0.20c_w$ plain flap set at 45°.

(a) Airfoil with flap.
(b) Flap alone.

FIGURE 41.—Section characteristics of the N. A. C. A. 23012 airfoil with a $0.20c_w$ plain flap set at 60°.

(a) Airfoil with flap.
(b) Flap alone.

FIGURE 42.—Section characteristics of the N. A. C. A. 23012 airfoil with a $0.20c_w$ plain flap set at 75°.

the slotted flap (figs. 3 to 9) was only partly stalled for high angles of attack at high flap deflections; whereas the upper surface of an external-airfoil flap (reference 5) was completely stalled for angles of attack above 3° at a flap deflection of 40°. The slotted flap taken as a whole was completely stalled (no increase in flap load with flap deflection) for a flap deflection between 40° and 50° (figs. 8 and 9), and the external-airfoil flap previously tested (reference 5) was completely stalled for a flap deflection between 30° and 40°.

The chord pressure diagrams for the slotted flap (figs. 10 to 15) are included because it is believed that relatively large forces probably existed that acted in a direction to retract this flap from its maximum-lift setting. As shown by these diagrams, the negative and positive components act in the same direction for nearly all of the arrangements tested except the 10° setting, so that the total chord pressure force is directed forward in practically all cases. These diagrams are considerably different from those of some Fowler flaps previously tested (reference 6), in which the negative and positive components acted in opposite directions and tended to counteract each other. It should be noted that the chord pressure forces do not include the skin-friction forces, which act nearly parallel to the chord and in such a way as to decrease the magnitude of the total chord force if negative or to increase it if positive.

No pressure-distribution tests were made to determine the effect of slight deviations of the flap from its optimum path. An analysis of the data presented in reference 1 and in this report, however, indicates that slight deviations from the optimum flap path would not be expected materially to affect the magnitudes and the distribution of the pressures over the flap. Any appreciable deviation from this optimum path would affect the total lift and the total drag of the airfoil-flap combination as noted in reference 1.

The distribution of pressures over the plain flap (figs. 16 to 24) is similar to that of a symmetrical plain flap reported in reference 9. High negative pressures for practically all angles of attack were found on the lower surface at the flap nose for flap deflections of −30° and −15° and on the upper surface for a flap deflection of 15°. For flap deflections above 15°, high negative pressures appeared on the upper surface at the flap nose. For flap deflections of 30° to 75° (figs. 21 to 24), the upper surface of the flap was stalled.

Comparison of pressure diagrams for the plain airfoil and for the airfoil-flap combinations at the *same lift* (figs. 25 and 26) shows the effect of the flaps. Increasing the flap angle and decreasing the angle of attack to maintain constant lift had the following effects: At the leading edge of the main airfoil, for both combinations, the magnitudes of the peak pressures were progressively reduced. At the trailing edge of the main airfoil, for the slotted-flap combination, the magnitudes of negative pressures were increased and the magnitudes of positive pressure were practically constant; whereas, for the plain-flap combination, the magnitudes of both positive and negative pressures were increased as the flap deflection was increased.

The flaps also obstructed the flow of air below the airfoil and caused the pressures to build up on the lower surfaces. The air flowing through the slot produced a high average velocity and increased the negative pressure on the upper surface of the slotted flap; the negative pressures on the upper surface of the plain flap changed very little.

The slotted flap had a pressure distribution similar to that of the plain airfoil, except for the double-peak pressures, indicating that, as long as the flap remains unstalled, it would have a small wake, as would the plain airfoil. Near the stall, however, the wake of the combination would still be small because of the slot effect, which permitted the attainment of high lifts with relatively low drag. This effect is absent for the plain flap on account of the large wake, especially near the stall.

Comparison of pressure diagrams for the plain airfoil and for the airfoil-flap combinations at the *same angle of attack* (figs. 25 and 26) shows that the flaps increased the negative pressure over the entire upper surface of the main airfoil and increased the positive pressure on the lower surface of the main airfoil except near the leading edge. The pressure gradients remained about the same except at the trailing edge of the main portion of the airfoil for the slotted-flap combination, where the adverse pressure gradients were decreased on the upper surface and increased on the lower surface. The pressures on the upper and lower surfaces of the flaps increased with flap deflection but more so for the slotted flap. The important effect of the flap, as shown by these diagrams, was its ability to influence the air flow around the main airfoil so that the airfoil carried a much greater load without stalling than was possible without the flap. The slotted flap was superior to the plain flap in this respect.

SECTION LOADS AND MOMENTS

The section coefficients are plotted in figures 27 to 42. Flap loads build up slowly for most lifts of the combination. The loads on the slotted flap increase more rapidly with flap deflection (figs. 27 to 33) than do the loads both on the plain flap (figs. 34 to 42) and on the external-airfoil flap (reference 5). The highest flap loads seem to be obtained with the slotted flap, the maximum normal-force coefficient being about 30 percent higher than for the external-airfoil flap. It is believed that slight deviations of the flap from its optimum path would not materially affect the flap loads. The greater part of the increment of normal-force coefficient of the combination due to deflecting the flaps downward, however, arises from the increased load carried by the main airfoil.

The chord-force coefficients of the slotted flap (figs. 28 to 33) are nearly all negative in sign; that is, the pressure forces parallel to the flap reference line are directed forward. The magnitudes of these forces are relatively high and considerably greater than those of some Fowler flaps of N. A. C. A. 23012 section that were recently tested (reference 6). The chord forces should be taken into account in design when consideration is being given to the resultant air loads acting on the slotted flap. As mentioned previously, the magnitudes of these forces would be somewhat decreased by the skin-friction forces that have not been included.

The pitching-moment coefficients of the slotted flap alone about its quarter-chord point were slightly higher than the pitching-moment coefficients of the external-airfoil flap (reference 5) for flap deflections up to about 30° (figs. 27 to 30). The pitching-moment center for both flaps was at about the same location. For a flap deflection of 40° (fig. 31), the pitching-moment coefficients for the slotted flap were much smaller than they were for the external-airfoil flap. For higher flap deflections, the pitching-moment coefficients increased quite rapidly (figs. 32 and 33). The hinge moments for the plain flap were high and increased rapidly with an increase in flap deflection (figs. 34 to 42).

CONCLUSIONS

1. These pressure-distribution tests show that, as with other types of flap, the greater part of the increment of total maximum lift due to deflecting the slotted flap downward arises from the increased load carried by the main airfoil.

2. The maximum normal-force coefficient for the slotted flap investigated had a higher value than that attained by other types of flap, and the magnitudes of the pressure chord-force coefficient were relatively large.

3. The pitching-moment coefficients for the slotted flap alone were slightly higher than the pitching-moment coefficients for an external-airfoil flap alone (moment centers had approximately the same location) for flap deflections up to 30°.

4. The pressure diagrams showed that, when the plain airfoil and airfoil-flap combinations were compared at the *same total normal-force coefficient*, the flap reduced the adverse pressure gradients and the tendency of the main airfoil to stall. The slotted flap was more effective in this respect than the plain flap or an external-airfoil flap.

5. The pressure diagrams showed that, when the plain airfoil and the airfoil-flap combinations were compared at the *same angle of attack*, the flap influenced the flow of air around the main airfoil so that the airfoil carried a much greater load without stalling than was possible without the flap. The slotted flap was more effective in this respect than the plain flap or an external-airfoil flap.

LANGLEY MEMORIAL AERONAUTICAL LABORATORY,
NATIONAL ADVISORY COMMITTEE FOR AERONAUTICS,
LANGLEY FIELD, VA., *March 17, 1938.*

REFERENCES

1. Wenzinger, Carl J., and Harris, Thomas A.: Tests of an N. A. C. A. 23012 Airfoil with Various Arrangements of Slotted Flaps in the Closed-Throat 7- by 10-Foot Wind Tunnel, to be published at a later date.
2. Kiel, Georg: Pressure Distribution on a Wing Section with Slotted Flap in Free Flight Tests. T. M. No. 835, N. A. C. A., 1937.
3. Ruden, P.: Versuche an einem Düsenflügel. Jahrbuch 1937 der Deutschen Luftfahrtforschung. S. 1 75–1 86.
4. Wenzinger, Carl J., and Harris, Thomas A.: Pressure Distribution over a Rectangular Airfoil with a Partial-Span Split Flap. T. R. No. 571, N. A. C. A., 1936.
5. Wenzinger, Carl J.: Pressure Distribution over an N. A. C. A. 23012 Airfoil with an N. A. C. A. 23012 External-Airfoil Flap. T. R. No. 614, N. A. C. A., 1938.
6. Wenzinger, Carl J., and Anderson, Walter B.: Pressure Distribution over Airfoils with Fowler Flaps. T. R. No. 620, N. A. C. A., 1938.
7. Harris, Thomas A.: The 7 by 10 Foot Wind Tunnel of the National Advisory Committee for Aeronautics. T. R. No. 412, N. A. C. A. 1931.
8. Platt, Robert C.: Turbulence Factors of N. A. C. A. Wind Tunnels as Determined by Sphere Tests. T. R. No. 558, N. A. C. A., 1936.
9. Jacobs, Eastman N., and Pinkerton, Robert M.: Pressure Distribution over a Symmetrical Airfoil Section with Trailing Edge Flap. T. R. No. 360, N. A. C. A., 1930.

TABLE I.—ORIFICE LOCATIONS ON AIRFOIL-FLAP COMBINATIONS TESTED

N. A. C. A. 23012 36-inch airfoil with a $0.20c_w$ plain flap		N. A. C. A. 23012 36-inch airfoil with a $0.2566c_w$ slotted flap			
Orifice locations on upper and lower surfaces in percent chord from leading edge		Orifice locations on upper and lower surfaces of main portion of airfoil in percent chord from leading edge		Orifice locations on upper and lower surfaces of flap in percent flap chord from leading edge	
Orifice	Location	Orifice	Location	Orifice	Location
0	0.00	0	0.00	0	0.00
1	1.25	1	1.25	1	1.25
2	2.50	2	2.50	2	2.50
3	5.00	3	5.00	3	5.00
4	10.00	4	10.00	4	10.00
5	20.00	5	20.00	5	18.00
6	30.00	6	30.00	6	30.00
7	40.00	7	40.00	7	45.00
8	50.00	8	50.00	8	62.50
9	60.00	9	60.00	9	72.50
10	70.00	10	67.00	10	82.50
11	75.00	11	70.00	11	92.50
12	78.00	12	74.00	----------	----------
13	80.00	13	78.00	----------	----------
14	82.50	14	81.50	----------	----------
15	85.00	----------	----------	----------	----------
16	90.00	----------	----------	----------	----------
17	95.00	----------	----------	----------	----------
18	98.00	----------	----------	----------	----------

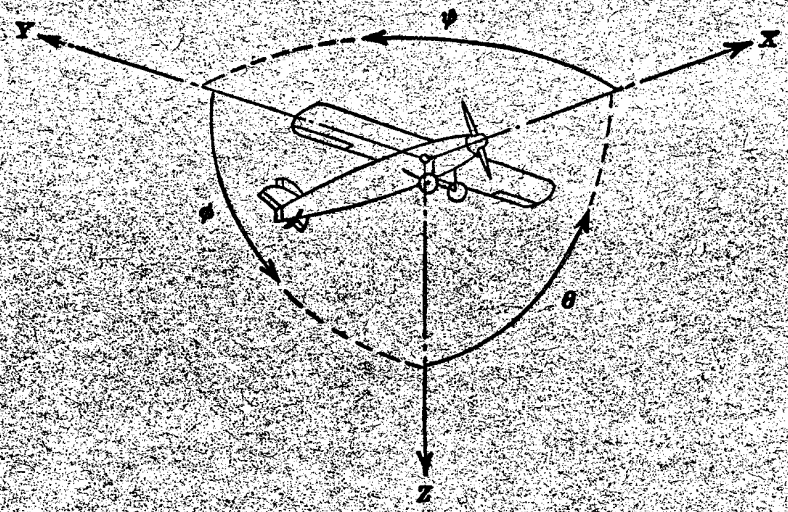

Positive directions of axes and angles (forces and moments) are shown by arrows

Axis		Force (parallel to axis) symbol	Moment about axis			Angle		Velocities	
Designation	Symbol		Designation	Symbol	Positive direction	Designation	Symbol	Linear (component along axis)	Angular
Longitudinal	X	X	Rolling	L	$Y \longrightarrow Z$	Roll	ϕ	u	p
Lateral	Y	Y	Pitching	M	$Z \longrightarrow X$	Pitch	θ	v	q
Normal	Z	Z	Yawing	N	$X \longrightarrow Y$	Yaw	ψ	w	r

Absolute coefficients of moment

$C_l = \frac{L}{qbS}$ (rolling) $\quad C_m = \frac{M}{qcS}$ (pitching) $\quad C_n = \frac{N}{qbS}$ (yawing)

Angle of set of control surface (relative to neutral position), δ. (Indicate surface by proper subscript.)

4. PROPELLER SYMBOLS

D, Diameter

p, Geometric pitch

p/D, Pitch ratio

V', Inflow velocity

V_s, Slipstream velocity

T, Thrust, absolute coefficient $C_T = \frac{T}{\rho n^2 D^4}$

Q, Torque, absolute coefficient $C_Q = \frac{Q}{\rho n^2 D^5}$

P, Power, absolute coefficient $C_P = \frac{P}{\rho n^3 D^5}$

C_s, Speed-power coefficient $= \sqrt[5]{\frac{\rho V^5}{P n^2}}$

η, Efficiency

n, Revolutions per second, r.p.s.

Φ, Effective helix angle $= \tan^{-1}\left(\frac{V}{2\pi r n}\right)$

5. NUMERICAL RELATIONS

1 hp.=76.04 kg-m/s=550 ft-lb./sec.

1 metric horsepower=1.0132 hp.

1 m.p.h.=0.4470 m.p.s.

1 m.p.s.=2.2369 m.p.h.

1 lb.=0.4536 kg.

1 kg=2.2046 lb.

1 mi.=1,609.35 m=5,280 ft.

1 m=3.2808 ft.

U. S. GOVERNMENT PRINTING OFFICE: 1938